Title
BETA DECAY OF THE LAMBDA HYPERON

Author
Singleton, William Joshua.

Publication Date
1964-05-05

Thesis/dissertation

UCRL-11432

University of California

Ernest O. Lawrence Radiation Laboratory

BETA DECAY OF THE LAMBDA HYPERON

Berkeley, California

DISCLAIMER

UCRL-11432

UNIVERSITY OF CALIFORNIA

Lawrence Radiation Laboratory
Berkeley, California

AEC Contract No. W-7405-eng-48

BETA DECAY OF THE LAMBDA HYPERON

William Joshua Singleton

May 5, 1964

Printed in USA. Price $2.00. Available from the
Office of Technical Services
U. S. Department of Commerce
Washington 25, D.C.

BETA DECAY OF THE LAMBDA HYPERON

Contents

BETA DECAY OF THE LAMBDA HYPERON

William Joshua Singleton

Lawrence Radiation Laboratory
University of California
Berkeley, California

May 5, 1964

ABSTRACT

Lambda hyperons were produced by stopping K^- mesons in the Berkeley 30-inch heavy-liquid bubble chamber filled with a 76% CF_3Br - 24% C_3H_8 mixture by weight. A total of 230 000 useful pictures was taken and scanned for decays of the type $\Lambda \rightarrow p + e^- + \bar{\nu}$ and for the normal decay mode $\Lambda \rightarrow p + \pi^-$. There were 192 000 Λ decays in the film. Three methods for identifying Λ_β decays were used. The most successful method of determining the branching ratio $r = (\Lambda \rightarrow p + e^- + \bar{\nu}) / [(\Lambda \rightarrow p + \pi^-) + (\Lambda \rightarrow n + \pi^\circ)]$ made use of the Λ_β decays with electron tracks that either stopped in the chamber or had high curvature. The remaining β-decay candidates were selected by kinematics or by δ rays. The best value obtained is $r = (0.82 \pm 0.13) \times 10^{-3}$.

The form of the Λ_β decay interaction was studied by measuring the distributions of proton transverse momentum and of the angle between the proton and electron projected on the plane normal to the Λ direction. Measurement errors and selection biases were folded into the theoretical distributions for different forms of the interaction. Comparison of the modified theoretical distributions with the experimental data shows that a pure tensor interaction is ruled out with 99% confidence.

Assuming the interaction to be only V and A, $|C_A / C_V| > 0.5$ with 99% confidence. Both V-A and pure axial vector interactions are compatible with the data.

I. INTRODUCTION

The twofold purpose of this experiment was to measure the branching ratio for lambda β-decay ($\Lambda \rightarrow p + e^- + \bar{\nu}$) and to investigate the form of the decay interaction.

A value for the branching ratio was first predicted by Feynman and Gell-Mann on the basis of a proposed universal V-A interaction.[1,2] Their hypothesis of "universality" stated that all weak interactions involving four fermions should have the same strength as well as the same form. Experiments on muon decay, nuclear β-decay, and μ capture seem to confirm the idea of "universality" if small deviations from theory are attributed to renormalization effects of the strong interactions.

Neglecting renormalization, Feynman and Gell-Mann calculated the branching ratio for Λ_β decay to be 16×10^{-3}. Early experiments on hyperon β-decay soon indicated that the prediction was about an order of magnitude too high.[3] A more recent experiment by Aubert et al.[4] gives a value of $(3.0^{+1.5}_{-1.2}) \times 10^{-3}$ for the branching ratio. The determination of the branching ratio in the present experiment, which has been published previously,[5] gives a value of $(0.82 \pm 0.13) \times 10^{-3}$.

The discrepancy between the predicted branching ratio and the experimentally found values has been commonly attributed to renormalization effects, which cannot be calculated because of the lack of an adequate theory for strong interactions. However, it is possible that the V-A form of interaction does not apply to hyperon β-decay or that the cocept of "universal strength" needs modification.

Recently, Cabibbo[6] has proposed a theory of leptonic decays of strange particles based on the octet version of unitary symmetry for strong interactions and the V-A theory for weak interactions. He uses a modified form of "universality" that introduces into the theory a parameter which must be determined by experiment. Sakurai[7] has interpreted recent experimental data and recalculated the value of the parameter previously evaluated by Cabibbo. He uses this parameter to relate the Λ_β decay rate to the ratio $|x|$ of the axial vector to vector coupling constants. A determination of the branching ratio will then lead to a definite prediction of the ratio $|x| = |C_A|/|C_V|$.

A theory by Cornwall and Singh[8] also relates the Λ_β rate to the ratio $|x|$, but with a different expression. An experimental determination of both the Λ_β decay branching ratio, r, and the ratio $|x|$ is necessary to test these different theoretical proposals.

Using the branching ratio found in the present experiment, $r = (0.82 \pm 0.13) \times 10^{-3}$, one obtains from Cabibbo's theory a value $|x| = 0.94 \pm 0.12$, i.e. nearly an equal mixture of V and A. Using the same value for the branching ratio in the theory of Cornwall and Singh, one obtains the value $|x| = 0.06 \pm^{0.11}_{0.06}$, i.e nearly pure vector.

Baglin et al.[9] have recently studied a sample of 92 Λ_β decays and concluded that a pure vector interaction is very unlikely. Their result is consistent with the prediction of Cabibbo's theory, but inconsistent with that from the theory of Cornwall and Singh.

The present experiment was done in collaboration with the high-energy physics group at University College London and several individuals contributed to the analysis of the branching ratio.[5] For completeness, all phases of the analysis are reported, although the independent work of the present author concerned mainly the determination of the branching ratio from the Λ_β decays identified by kinematics, and the study of the form of the interaction.

The first part of this paper describes three methods for identifying lambda beta-decays. The branching ratio is calculated separately from the events found by each method. The second part describes the study of the form of the interaction using the proton momentum spectrum and angular correlations in the laboratory system.

II. EXPERIMENTAL PROCEDURE

A. Exposure

Approximately 300 000 Λ hyperons were produced in the Berkeley 30-inch propane-freon bubble chamber[10] by a beam of stopping K^- mesons. The chamber was in a 13 KG magnetic field and was filled with a mixture of 24% C_3H_8--76% CF_3Br by weight. This mixture was a compromise between a medium in which accurate momentum measurements could be made, and one in which electrons could be easily identified. The composition of the mixture was checked by measuring its density. This was done by removing a small sample of the liquid at operating conditions, measuring the density in the gaseous phase, and allowing for the ratio of expansion. A check on the density was made by using it as a free parameter in the range-energy relations and constraining the Λ mass to 1115.36 MeV. For this a sample of $\Lambda \rightarrow p + \pi^-$ decays in which both secondaries stopped were used. The properties of the chamber liquid are summarized as follows:

Properties of the C_3H_8--CF_3Br Mixture

Percentage composition	24% C_3H_8--76% CF_3Br
Operating temperature	37° C
Operating pressure	283 lb/in^2
Density (at operating conditions)	0.89 g/cc
Radiation length	22.5 cm

The K^- beam, designed by Murray et al.,[11] had a momentum of 800 MeV/c. This momentum was reduced so that the K^-'s would stop in the chamber and produce a maximum number of hyperons. The Λ's, produced by the interaction K^- (at rest) + nucleon $\rightarrow \Lambda$ + fragments, had relatively low momenta and therefore gave easily identifiable decay products.

The momentum of the K^- mesons was first reduced to 550 MeV/c by copper absorber placed directly before the chamber. It was further reduced to 440 MeV/c by a one-inch copper plate inside the chamber, five inches from the entrance. Two-thirds of the K^- mesons interacted at rest and most of the others interacted in flight.

To allow good ionization measurements, the chamber was operated so that minimum ionizing tracks had 7 to 10 bubbles per cm. However, electrons could not be distinguished from pions by ionization because of the relativistic rise in electron-track bubble density. Gap-length measurements yielded 1.2 to 1.3 x minimum ionization for 100 MeV/c electrons. This is indistinguishable from the 1.3 to 1.5 for pions between 140 and 200 MeV/c, the most probable momentum range for those pions that did not stop in the chamber.

A total of 230 000 useful pictures was obtained with an average of about three K's per picture.

B. Scanning Procedure

All of the film was scanned for the normal decay mode, $\Lambda \rightarrow p + \pi^-$, as well as for the Λ_β decay mode, $\Lambda \rightarrow p + e^- + \bar{\nu}$. Both types of events were required to have a visible production origin.

Normal Λ decays were identified by comparing scan-table measurements of momenta, angles, and ionization with kinematic curves. Each event was recorded, but only those with a negative track longer than 15 cm and leaving the chamber were measured on a "Franckenstein" or a digitized microscope. The measured events, which represented about 2% of those recorded, were processed by the FOG-CLOUDY-FAIR data reduction programs.[12] Events which turned out to be inconsistent with the assumption of a normal Λ decay were examined further as possible Λ_β decays.

Lambda beta-decays were recognized at the scan-table either by the electron track characteristics of high curvature and large δ rays or by the special kinematics of the decay. They were selected by one of the following criteria: (a) The vector $\vec{R}$ from the point of decay to a point along the negative track passed through a maximum value (Fig. 1); (b) the negative track was longer than 15 cm, left the chamber, and had a δ ray greater than 1 cm, as measured in a scan-table projection; (c) the negative track left the chamber and was too long for a Λ mesonic-decay as calculated from the proton momentum and opening angle. Events selected by criterion (a) will be called "R_{max} events". Eighty percent of these had electrons that stopped in the chamber. Those selected by criterion (b) and (c) will be called "δ ray events" and "kinematic events", respectively.

All events interpreted as β-decays at the scan-table were measured and rejected if found inconsistent with this interpretation. Measurements of the electron momenta were sufficiently uncertain so that the test was primarily on the transverse momenta of the protons.

To determine the scanning efficiency for the normal Λ decays, 10% of the film was scanned a second time. By comparing the two independent scans, and assuming that all events were found with the same probability, the efficiency was calculated to be 0.89 ± 0.01. However, if certain decay configurations were often missed, the calculated efficiency would be too high. The most difficult configurations to identify were ones with a very short proton or with the pion and proton colinear. If these were consistently missed, the bias would be at most 3%. To check that the scanners were not accepting a large percentage of background events, the second scanner noted questionable events which were found in the first scan. Examination of these events revealed that, on the average, 2.5% of the events accepted as normal Λ decays were spurious events. This estimate agreed with the percentage of events failing the constraints program from a random sample of about 1 000 events identified as normal Λ decays.

About 50% of the film was rescanned just for the R_{max} type of β-decay. To determine the efficiency of the second scan, each scanner was given film containing events found by others in the first scan. The average efficiency of both scans was 0.87 ± 0.05.

The scanning efficiency for β-decays with δ rays was determined by rescanning film that contained many of the events identified by δ rays on the first scan. The average efficiency for δ ray events was found to be 0.67 ± 0.15

The efficiency for recognizing Λ_β decays by kinematics was determined in a similar way. This efficiency was found to be 0.90 ± 0.07.

The first two columns of Table I list the number of events found in each category and the corresponding scanning efficiencies. The three groups of events were kept distinct and analyzed separately throughout the experiment.

C. Background

There were several sources of background to the Λ_β events. Some were large and difficult to estimate, but these could be eliminated by further acceptance criteria. The remaining sources of background could be calculated and subtracted. Some sources of background simulated all three types of β-decays, whereas others affected only one type.

A fraction of the Λ_β decays have a very short proton track. These can be simulated by asymmetric electron pairs in which the positron is too short to be distinguished from a proton. This background was eliminated by accepting only Λ_β decays in which the proton track was longer than 2 mm.

Lambda beta decays can also be simulated by events caused by a neutron striking a carbon nucleus which subsequently emits a proton and then β-decays. The highest energy electron from such a process is 13.6 MeV from the decay of an exited state of B^{12}. Electrons with this energy have a maximum range of 8.5 cm. These events were excluded by accepting only those β-decays with electrons longer than 9 cm.

The fraction of real Λ_β decays excluded by the selection criteria on the proton- and electron-track lengths, is 0.10 ± 0.03. To calculate this, the measured Λ-momentum spectrum (Fig. 2) was used in a relativistic three-body phase-space calculation. The 3% error reflects the uncertainty in the Λ-momentum spectrum and in the C. M. electron momentum spectrum.

The next few sources of background which were considered turned out to be unimportant in this experiment. Some of the Λ_β decays emitted protons which left the chamber. It is possible that this type of event could be simulated by a K_2° decay, or by a μ^- entering the chamber through the top or bottom glass and emitting an electron near a K^- interaction. Fifteen events had protons leaving the chamber, but each could be identified as a β-decay by the ionization of the positive track.

Another possible background could come from neutron stars consisting of a proton and a π° which emits an asymmetric Dalitz pair in which the positron is not seen. The visible proton and electron tracks would appear to come from a Λ_β decay. The chance of a positron from the Dalitz pair being less than 0.3 MeV and, hence, passing unseen is about 4×10^{-3}; adding to this a 1×10^{-3} chance that the positron will annihilate in the first millimeter, gives the total chance of missing the positron as 5×10^{-3}. One in 80 π°'s emit a Dalitz pair, so the probability that such a neutron star will simulate a Λ_β decay is 6×10^{-5}. A search for electron pairs pointing back to proton recoils led to an estimated total of 200 neutron stars emitting π° mesons. This background, therefore, would be only one event in about 10^4 Λ_β decays.

A γ ray from the type of neutron star just mentioned could produce a Compton electron near its origin. Such an event would be similar to a Λ_β decay. Observation of Compton electrons pointing back to proton recoils provided an estimate of 1% for this background.

Two percent of the pions from normal lambda decay emit muons in flight and two-thirds of these muons emit electrons after coming to rest. Such events may have the general appearance of a Λ_β decay, but the dark track of the stopping muon always contrasts sharply with the light track of the electron. Usually there is also a kink between the muon and electron tracks, and one has no trouble in distinguishing these events from Λ_β decays. There are some cases where the pion in flight emits the muon in the opposite direction so that the μ has no detectable range in the chamber. The decay electron would then appear to be a continuation of the pion track. Only slow pions can emit muons nearly at rest in the lab system. These pions have an ionization of at least 2.5 times minimum for a distance of 1 cm before the decay point, and the change in ionization after that point can be easily seen.

A further conceivable contamination from these Λ decays with a π-μ-e sequence is the case where the lines of flight of the π and μ are opposite to that of the proton. If the π and, hence, the μ had very low momentum their tracks could appear to be part of the proton track, so that only the proton and the decay electron would be recognized. For one of these events to cause confusion the π must make an angle greater than 170° with the proton and have a momentum less than 45 MeV/c. With these limits, this background is calculated to be much less than one event in the film.

The sources of background outlined so far are expected to give less than two spurious events in the experiment.

The main source of background for the δ ray events was caused by the stray Compton electrons in the chamber. Such a Compton electron originating near a π track may appear to be a δ ray on an electron track. To cause confusion, the Compton electron must begin within some effective volume around the π track. The size of this volume was estimated by studying the subjective acceptance criteria for δ rays. The average effective volume for pions with lengths exceeding 15 cm and leaving the chamber was found to be 0.6 cm^3, which is 1.6 x 10^{-5} the total volume of the chamber. An average of 35 Compton electrons were found per picture, so the probability that one of these pions has a simulated δ ray is about 1 in 1 800. This result agrees with that found by scanning for simulated δ rays on stopping pions, K mesons, and protons, where δ rays of 1 cm are impossible. The background was calculated to contribute 17% of the events identified by the δ ray method.

The major background for the kinematic events came from mesonic Λ decays in which the π emitted a μ in the forward direction and the μ left the chamber. In such a case the total length of the negative track may be longer than the permitted π range. To estimate this background, a Monte Carlo program was written to simulate $\Lambda(\pi \rightarrow \mu)$ events which satisfied the scanning criteria for kinematic Λ_β decays. The results revealed a large background that depended strongly on subjective scanning criteria. Due to the difficulty in calculating this contamination, stricter acceptance criteria were adopted for the kinematic events. These criteria, described later, selected a background-free sample of kinematic Λ_β decays and allowed a simple estimate of the excluded fraction.

A background still remained due to neutron stars that produced a proton and π^- simulating the Λ_β kinematics. Film was scanned for neutron stars of this type that were not associated with acceptable origins. A lifetime cutoff was used to select these events. Geometric factors were then used to determine the background of neutron stars that would simulate Λ_β's by occuring near a K^- interaction. This was found to be 1.7 events, i.e. 10% of the number of events in the category.

III. DETERMINATION OF THE BETA DECAY BRANCHING RATIO

A. Introduction

Because the three independent means for identifying Λ_β decays have different detection efficiencies, the branching ratio has been calculated separately in each case. Our general procedure was to apply corrections to the number of events observed, for scanning efficiency, for the selection bias introduced by the minimum track length requirements, and for the effects of background. The detection efficiency of the chamber was then calculated for the three categories, and the total number of β-decays was determined from the observed number.

The branching ratio, r, is defined here as the ratio of the number of Λ_β decays to the number of Λ mesonic decays. Assuming that two-thirds of the Λ mesonic decays go via the charged mode,[13] the total number of Λ mesonic decays in the experiment was found to be 322 000 ± 10 000. The error includes the statistical error, the error in scanning efficiency, and the maximum effect of the scanning biases mentioned on p. 6.

B. Branching Ratio From R_{max} Events

To determine the fraction of all Λ_β decays that exhibit the R_{max} property in the chamber (described on p. 5), a Monte Carlo program, written by D. J. Miller,[14] was used to simulate the formation of electron tracks from Λ_β decays. The program initiated electrons from the co-ordinates of a random sample of 208 normal Λ decays found in the chamber. The direction of the e^- was chosen at random, which was justified by the observation that the pions from normal Λ decays showed no detectable correlations with any direction in the chamber. The initial energy of each electron was chosen from an energy spectrum (Fig. 3) derived by folding the Λ-momentum distribution of Fig. 2 into a phase-space electron-energy spectrum in the center-of-mass system. Six tracks of different energies and directions were initiated from each origin.

The tracks were generated in consecutive segments of 0.9 cm, and four effects were simulated in each segment. First an energy loss due to collision was evaluated, taking into account the energy at the beginning of the segment. Next, the magnetic bending corresponding to the momentum and dip angle was calculated. Finally, random choices were made of both multiple scattering and Bremsstrahlung energy loss. At the end of each segment a new energy, position and direction were computed and a further segment begun. This process continued until either (1) the energy dropped below 1.5 MeV and the particle was considered to have stopped, or (2) the track passed through R_{max}. The final energy of electrons, the detection efficiency as a function of dip angle and of initial electron momentum, and the total track lengths were compiled and printed.

The theory used for collision loss was that of Sternheimer.[15] The radiation loss was calculated from Heitler's analytic formula[16] using the exact cross-sections given by Koch and Motz,[17] and the multiple scattering theory is that described by Barkas and Rosenfeld.[18]

The program was checked against the behavior of a sample of electrons with a known energy spectrum, provided by μ mesons that stopped in the chamber and decayed. The co-ordinates of the origin, the initial direction of the electron, and the value of R_{max} (if existing) were recorded for 170 of these μ^- decays without any restriction on the electron dip angle. It was observed that $(62 \pm 6)\%$ of the electrons went through a maximum radius vector. The program predicted $(65.5 \pm 2.5)\%$ using the same origins and an electron spectrum given by the two component neutrino theory ($\rho = 0.75$).[1] The observed and calculated mean values of R_{max} were 6.80 cm and 6.95 cm respectively, and the shapes of the distributions of R_{max} were found to agree well.

This confirmation of the accuracy of the program for electrons of energy less than 50 MeV was satisfactory from the point of view of its application to the generally higher energy electrons from Λ_β decay since the main uncertainty was due to Heitler's approximation for Bremsstrahlung below 40 MeV. In addition, runs of the program were made with small changes in the values of the radiation loss, collision loss, and magnetic field. Also, runs were made without multiple scattering. In every case the effect on the detection efficiency was small.

The detection efficiency for R_{max} events having negative secondaries with dip angle < 30°, was found to be 0.60 ± 0.02. The error arises from the statistics on the number of Λ decay origins fed into the program. The dip angle requirement was found to be necessary in practice because steeply dipping electrons that pass through R_{max} can be confused with stopping pions. The requirement removes half of the total number of Λ_β decays from consideration by excluding half of the total solid angle.

The number of events detected by the R_{max} criterion and satisfying the dip angle requirement was 62 and the scanning efficiency for these events was 0.87 ± 0.05. The correction of 0.10 ± 0.03 had to be applied for events excluded by the requirement that the range of the proton should be > 2 mm and that of the electron > 9 cm. The Monte Carlo Program described here was used to obtain the part of this correction due to electron tracks being too short. This contribution amounted to 4%. When these various factors were taken into account, the number of leptonic decays was estimated to be 62 / (0.60 x 0.50 x 0.87 x 0.90) = 264 ± 40. Dividing this by the total number of Λ decays, 322 000 ± 10 000, the branching ratio becomes $\bar{r}$ = (0.82 ± 0.13) x 10^{-3}.

C. Branching Ratio From δ Rays

Events with negative secondaries leaving the chamber and having δ rays greater than 1 cm were recorded as possible Λ_β decays. The cutoff of 1 cm was chosen because only 1.5% of the pions from normal Λ decay have enough velocity to produce such a δ ray. For each δ ray event the proton momentum and the opening angle were used to calculate the pion momentum corresponding to mesonic Λ decay. Events were rejected for which this pion momentum was sufficient to produce a δ ray of the observed length.

To insure reasonable scanning efficiency, the δ ray events were required to have negative tracks longer than 15 cm. Twelve events of this type were found. The total number of Λ_β's was deduced from these events by assigning to each a weighting factor equal to the inverse of the probability that its electron should have produced a δ ray of the required length. The weighting factor is $[1 - \exp(-\ell/\lambda)]^{-1}$, where ℓ is the electrons's path length and λ is the mean free path for producing these δ rays.

In practice it was necessary to use the horizontal projection of the δ ray, since multiple scattering makes it practically impossible to measure the length in space. Thus, λ in the expression for the weighting factor does not have its conventional meaning. Its value was determined by scanning for δ rays on high-energy electron pairs.

The weighting factor method was checked by applying it to the R_{max} events (with no electron dip angle cutoff) which happened to have δ rays. There were 29 R_{max} events with δ rays and their weighting factors predicted there should be altogether 69 ± 14 R_{max} events.

There were actually 79 R_{max} events, which is very consistent with the prediction.

A background of 2.1 events due to stray Compton electrons, estimated on p. 11, was subtracted from the 12 observed events leaving 9.9 δ ray events. These had an average weighting factor of 2.5 which implies that 40% of the decays with tracks longer than 15 cm and leaving the chamber before passing through R_{max} have δ rays. The Monte Carlo program for simulating electron tracks has computed that $(18 \pm 4)\%$ of Λ_β decays will have such a length of negative track. Allowing, further, for 6% of all events lost because the proton range was less than 2 mm and for the scanning efficiency of 0.67 ± 0.15, the observed δ ray events represent $(4.4 \pm 1.5)\%$ of all decays. The branching ratio from the δ ray events is then $r = (0.70 \pm 0.31) \times 10^{-3}$.

D. Branching Ratio From Kinematics

Some of the Λ_β decays that cannot be detected by the R_{max} or δ ray methods can be identified by kinematics. The problem is to eliminate the background coming mainly from normal Λ decays in which the negative secondary leaves the chamber. The Λ_β, being a three-body decay with one invisible decay product, differs from the two-body decay in that the two visible tracks will not in general balance transverse momentum or lie in the same plane with the Λ line-of-flight. However, these differences cannot be used with confidence to separate Λ_β decays from mesonic Λ decays, mainly because some Λ's scatter before decaying. For scattered Λ's with no visible recoil the measured line-of-flight is wrong, and the two-body kinematics appears to be inappropriate. This is the reason for adopting the requirement that the negative track length be greater than that calculated for a normal Λ decay using the proton momentum and opening angle. This criterion does not depend on the Λ line-of-flight measurement.

To eliminate the further background of $\Lambda(\pi \rightarrow \mu)$ decays, one must determine the maximum negative track length $(\ell_\pi + \ell_\mu)$ from such a decay, and require the kinematic events to have a yet longer negative track. First, all candidates were required to have a negative track length of at least 15 cm. For a normal Λ decay to have a 15 cm negative track it must emit a pion with a lab momentum of at least 100 MeV/c and this pion must immediately emit a μ in the forward direction. Therefore, events with configurations that would accompany π momenta of less than 100 MeV/c, but have have negative tracks greater than 15 cm, are clearly not $\Lambda(\pi \rightarrow \mu)$ decays. Separation of the background was done by plotting all prospective kinematic events on a diagram similar to Fig. 4. In this plot the opening angle is on the ordinate and the proton momentum on the abscisa. The line is the curve of constant pion momentum equal to 100 MeV/c for normal Λ decay. All $\Lambda(\pi \rightarrow \mu)$ events with negative tracks longer than 15 cm fell below the line, and the events falling in the region above were accepted as Λ_β decays.

Monte Carlo β-decays were likewise plotted and 0.47 ± 0.04 of them fell in the background-free region. It has been estimated previously that 0.18 ± 0.4 of all Λ_β decays have an electron length of 15 cm and leave the chamber before going through R_{max}. The correction for the proton length cutoff of 2 mm is much less than one event in the background-free region. Seventeen events were found with a scanning efficiency of 0.90 ± 0.07. A 10% neutron star background had to be subtracted, leaving an equivalent of 15.3 events. These represent $(7.6 \pm 2.7)\%$ of the total number of Λ_β decays in the film. From kinematic events the branching ratio is $r = (0.62 \pm 0.22) \times 10^{-3}$.

E. Discussion Of Branching Ratio

The quoted branching ratios depend on our assumption of the shape of the laboratory electron momentum spectrum because the detection efficiency is not the same for all momenta. The electron momentum distribution used (Fig. 3) was obtained by folding the lambda momentum distribution (Fig. 2) into a three-body Lorentz-invariant phase-space calculation. The total detection efficiency determined from this distribution differs by less than 1% from that determined from the vector, axial vector, scalar, or tensor interactions (assuming no "induced" for factors). Therefore, the branching ratios we obtain will remain within the quoted errors for any of the above spectra.

The branching ratios obtained by the R_{max} and the δ ray and kinematic methods are in good agreement, even though the shapes of their detection-efficiency curves (Fig. 5) are different. However, due to the large errors on the δ ray and kinematic ratios, little can be inferred about the validity of the assumed electron momentum spectrum, except that it is consistent with the results, and very large deviations from it are unlikely.

IV. FORM OF THE LAMBDA BETA DECAY INTERACTIONS

A. Introduction

The second purpose of the experiment was to study the form of the Λ_β decay interaction. The analysis has been confined to quantities measured directly in the laboratory system. Information obtained from quantities calculated in the Λ rest system is being studied at University College London and will be reported elsewhere.

To determine the C.M. quantities, one must first measure the Λ direction, the proton momentum, and the electron momentum. Assuming no measurement error, one can then calculate the momentum of the neutrino in the laboratory and perform the Lorentz transformation to the Λ rest system. However, there are generally two distinct solutions for the neutrino momentum and no way of choosing which one is correct. Moreover, when measurement errors are present, there may be no possible solution for the neutrino, and it becomes necessary to adjust the measured quantities (in a least squares fashion) in order to obtain an approximate solution. This would be necessary if, for instance, the electron or proton transverse momentum were measured to be greater than the theoretical maximum of 163 MeV/c. Forty- to fifty-percent of the decays must be adjusted for the C.M. analysis.

The problems just mentioned are not encountered in the present analysis, which involves only the proton transverse momentum (P_t) and the projected angle Φ between the proton and the electron in the plane perpendicular to the Λ direction (Fig. 6). As will be shown later, these quantities are sensitive to the form of the interaction, and they contain no ambiguities due to the two solutions. Furthermore, no procedure for "fitting" is necessary.

The general procedure for determining the form of the coupling was to compute the theoretical distributions of P_t and Φ for several interactions and then to modify them by folding in measurement errors and selections biases. Finally the experimental results were compared with the modified theoretical distributions in an attempt to determine the most probable form of the interaction.

B. Possible Forms Of The Interaction

The number of Λ_β decays in this experiment is insufficient for a detailed study of the weak interaction. Therefore, in the consideration of the different possible interactions, the contributions of the "induced" form factors have been neglected. The expressions for these interactions have been worked out in a convenient form by L. Egardt.[19]

The S-matrix element for the weak interaction is written:

$$S = \frac{G}{\sqrt{2}} (2\pi)^4 \, \delta \, (P_\Lambda - P_p - P_e - P_\nu) \sqrt{\frac{m_\Lambda \, m_p \, m_e}{E_\Lambda \, E_p \, E_e \, E_\nu}} \cdot M \qquad (1)$$

where G is the weak coupling constant and M is the matrix element for the particular couplings given below.

Vector and axial vector coupling:

$$M = \bar{u} \, (P_p) \, \gamma_\mu \, (C_V + \gamma_5 \, C_A) \, u \, (P_\Lambda) \cdot \bar{u} \, (P_e) \, \gamma_\mu \, (1 + \gamma_5) \, v \, (P_\nu) \qquad (2)$$

C_V and C_A are, respectively, the vector and axial vector form factors and are assumed to be constants.

Scalar-pseudoscalar coupling:

$$M = \bar{u} \, (P_p) \, (1 + \gamma_5) \, u \, (P_\Lambda) \cdot \bar{u} \, (P_e) \, (1 + \gamma_5) \, v \, (P_\nu) \qquad (3)$$

Tensor coupling:

$$M = \bar{u} \, (P_p) \, \sigma_{\mu\nu} \, (1 + \gamma_5) \, u \, (P_\Lambda) \cdot \bar{u} \, (P_e) \, \sigma_{\mu\nu} \, (1 + \gamma_5) \, v \, (P_\nu)$$
$$\sigma_{\mu\nu} = \frac{1}{2i} (\gamma_\mu \, \gamma_\nu - \gamma_\nu \, \gamma_\mu) \qquad (4)$$

The decay rate is given by:

$$\Gamma\,(E_p, E_e)\,dE_p\,dE_e = |G|^2\,(2\pi)^3\,\frac{1}{16m_\Lambda}\,|M|^2\ , \tag{5}$$

and the expressions for $|M|^2$ are given below in terms of the proton and electron energy in the Λ rest system.

Vector and axial vector coupling:

$$|M|^2 \propto -(1+x^2)\,E_e^2 + AE_e + B \tag{6}$$

where

$$A = \frac{1}{2m_\Lambda}\left[(1+x^2)\,(2m_\Lambda^2 + m_e^2) + 2x\,(m_\Lambda^2 + m_p^2)\right] - (1+x)^2\,E_p$$

and

$$B = -\frac{1}{2}\,(1+x)^2\,E_p^2 + \frac{1}{4m_\Lambda}\left[(1+x)^2(3m_\Lambda^2 + m_p^2 + m_e^2) + \frac{m_p}{2}(1-x^2)\right]E_p,$$

and where $x = C_A/C_V$ is the ratio of the axial vector to the vector coupling constant.

Scalar coupling:

$$|M|^2 \propto \frac{E_p}{2m_\Lambda}\,(m_\Lambda^2 + m_p^2 - m_e^2) - E_p^2 \tag{7}$$

Tensor coupling:

$$|M|^2 \propto -4E_e^2 - 2E_e\left[2E_p - \frac{1}{m_\Lambda}\,(2m_\Lambda^2 + m_e^2)\right] \tag{8}$$

$$- E_p^2 + \frac{E_p}{2m_\Lambda}\,(5m_\Lambda^2 + m_p^2 + 3m_e^2) - (m_\Lambda^2 + m_p^2 + m_e^2)$$

To determine the coupling, it is clear that one must choose independent variables which are sensitive to changes in the matrix element and which can be accurately measured. On both counts the electron energy is a poor choice. The phase-space factor dominates the shape of the electron spectrum[20] and the measurement errors are typically ±40%. Figure 7 shows the predicted E_e spectrum for vector and scalar, which are the extreme cases; those for tensor and mixtures of V and A lie in between. One is clearly unable to distinguish these small differences in spectra with the present techniques.

Egardt has pointed out that, in the Λ rest frame, the distribution of the proton momentum and the angle between proton and electron are dependent on the type of coupling. This can be seen from the curves in Fig. 8 and Fig. 9. The projections of these two quantities on the Λ transverse plane (Fig. 13) retain much of the sensitivity to the interaction and can be measured directly in the laboratory system. Therefore, these are the variables which have been chosen for studying the decay interaction.

C. Selection And Measurement Of Events

To study the form of the interaction, only the R_{max} events have been used, including those with electron dips greater than 30°. The dip angle cutoff was necessary in measuring the branching ratio because in some cases steep electrons are confused with pions. However, most of the "steep events" could be clearly identified as Λ_β decays; the questionable ones were all eliminated by the additional criteria (imposed for other reasons) which will be described in this section.

Beta decays identified by kinematics were not used because the selection criterion imposed on the proton momentum and opening angle introduced a large bias. The δ ray events, which were found with relatively low scanning efficiency, were also excluded from the analysis. Although they contain no apparent bias, the advantage of using events all selected on the same basis was considered sufficient reason to leave out these 12 events. The initial sample of R_{max} events, including all electron dip angles, consisted of 79 events.

A study of the measurement errors has shown the need for further restrictions on the beta decays to insure reliable measurements. It has also provided the necessary information for simulating these errors with Monte Carlo programs which were used in the later analysis.

First, the microscope setting error was determined on the R_{max} events. This was done by carefully measuring each event twice and taking the deviation of corresponding measurements. The r.m.s. setting error on these events was found to be 130_μ, which is 30% smaller than that of normally measured lambdas. Because of the similarity between the two types of events, this difference was attributed to the special handling of the Λ_β decays.

The r.m.s. errors for dip angle α and asimuthal angle β are calculated in the FOG program by the following expressions:

$$d\alpha = \left[\frac{a_2 (P^2 + m^2) L\alpha}{(P^2 \sin\alpha) P^2} + \frac{a_3 \sin^4\alpha}{L_\alpha^2} \right]^{\frac{1}{2}} a_5 \qquad (9)$$

$$d_\beta = \left[\frac{a_2 (P^2 + m^2) L_\beta}{(P^2 \sin\alpha)^2 \sin\alpha} + \frac{a_4}{L_\beta^2} \right]^{\frac{1}{2}} a_6 \quad .$$

The constants are defined by:

$a_2 = (55/X_0) \times 10^2$ (X_0 is the radiation length) (10)

$a_3 = 2e_z^2 \times 10^4$

$a_4 = 2e_x^2 \times 10^4$

$a_5 = a_6 = 10^{-2}$ (may be adjusted empirically),

where e_x is the setting error in the horizontal plane and e_z is the corresponding error in the vertical direction. L_α and L_β are the lengths of track used in calculating α and β, respectively; they are chosen so that $d\alpha$ and $d\beta$ will be minimal. In expressions (9) and (10) the first term is the multiple scattering error and the second term is the measurement error. The multiple scattering term is, of course, dropped in the calculation of $d\alpha$ and $d\beta$ of the Λ line-of-flight.

Measurement errors are comparitively large for short tracks. With the use of eq. (9) the error $d\alpha$ has been plotted (Fig. 10) as a function of length for a) the proton track, and b) the Λ line-of-flight. Curve a) was calculated by varying the momentum, P, and using the corresponding proton range for L_α. Curve b) shows the error in α from microscope setting errors at the production and decay origin.

If these curves are a true representation of the errors for short tracks, it appears necessary to introduce a minimum length criterion, for both the proton and Λ, to insure reliable measurements. This is all the more necessary because very short tracks can be confusing to the measurer and it is expected that the formulae underestimate the errors in these cases. Therefore, each β-decay was required to have a proton track length (ℓ_p) and a Λ line-of-flight (ℓ_Λ) at least 0.5 cm.

Multiple scattering prevented accurate momentum measurements by curvature. In particular, the proton momentum had a typical error of >100% when measured by curvature, but an error of only 3% when measured by range. Since it was important to measure this momentum accurately for determining P_t, all events were required to have stopping protons.

The criteria of stopping protons and minimum track lengths reduced the original sample of 79 to 50 events.

D. Simulation Of Λ_β Decays

The measurement errors and selection biases had to be folded into the theoretical distributions of P_t and Φ before these distributions could be compared to the data. This was done by a computer program which generated lambda beta decays according to a given theory, and then altered them by simulating experimental conditions. The following is a brief description of the program.

The program generated β-decays using the data from a random sample of 770 Λ's found in the chamber. The Λ momentum, direction, and the coordinates of the decay point were read into the program, which then generated a large number of β-decays from each lambda.

Decays were initiated in the C.M. system by choosing random values for the kinetic energy of the proton and electron. Following the two random choices of energy, the neutrino energy was calculated from total energy conservation and the three corresponding C.M. momenta were determined.

Momentum conservation then determined the relative C.M. angles provided the three momenta formed the sides of a closed triangle. A test was made to see if any one of the three momenta was greater than the sum of the other two; if so, the decay was rejected and a new decay initiated.

Once the triangle test was passed and the relative C.M. angles were computed, the matrix element subroutines were "called" by the main program. There were four of these subroutines; two represented mixtures of V and A (one went from V to V-A, and the other from V-A to A); the other two represented the scalar and tensor interactions.

These subroutines contained the matrix elements expressed in terms of the proton and electron energies as in eqs. (6) to (8) and were normalized to have a maximum value of unity. Each subroutine made a "pass" or "fail" decision which was weighted by the probability for the particular energies to occur. To do this, the value of the matrix element was calculated and then a random value was chosen between 0 and 1. If the random value was greater than the calculated value, the decision was "fail"; otherwise it was "pass". Altogether there were nine different interactions used by the program. For each decay they were "called" in succession and the "pass - fail" decisions were recorded. At this point, if all nine decisions were "fail", the decay was rejected, but if any one was "pass", the event was continued.

The next step was to give the C.M. decay plane a random orientation in space and to transform the decay to the laboratory system using the momentum and direction of one of the measured Λ's. The chamber geometry was then introduced and the event was given the decay point coordinates of this Λ.

The effect of the non-uniform detection efficiency for R_{max} events was next introduced into the program. A "detection" subroutine, containing the efficiency curve (Fig. 5) in terms of laboratory electron energy, made a "pass" or "fail" decision. The events that passed contained our experimental bias against high energy electrons.

Using range-energy relations, the program computed the end point of the proton track (assuming a straight line), and rejected the event if this point lay outside the chamber. Next, the proton range requirement of >0.5 cm was applied by requiring the momentum to be >185 MeV/c. Finally, ℓ_Λ was calculated using the known Λ momentum and a lifetime chosen at random from an exponential distribution. An event with ℓ_Λ<0.5 cm was rejected.

Having passed all of the selection requirements, the event was altered in accordance with the experimental errors. The errors in α and β were assumed to have normal distributions with standard deviations given by eqs. (9) and (10), and the r.m.s. error of the proton momentum was taken to be 3%. For each track, errors were chosen at random from these distributions and applied so that an event was obtained as it would appear after measurement.

Finally, the quantities P_t and Φ were calculated and the event was recorded. There were, of course, nine groups in which the event could be recorded, corresponding to the nine matrix elements. It was not recorded in a group whose matrix element subroutine gave a "fail" decision.

The change in the P_t and Φ spectra caused by the separate effects of detection efficiency, cutoffs, and experimental errors can be seen in Fig. 11 and Fig. 12. First, 12 000 β-decays were generated (using a V-A matrix element) without imposing experimental effects. Five subsequent groups of events were generated, each differing from the previous group by one additional experimental effect. The P_t and Φ spectra show the result of "turning on" the following effects in succession: electron energy bias, stopping proton requirement, minimum track length cutoffs, multiple scattering and measurement errors.

The bias in electron energy, though large, had no significant effect on the distribution of P_t. Minimum track-length cutoffs caused the largest change in the mean of the P_t-spectrum, but multiple scattering and measurement errors also tended to shift the mean upward as well as to broaden the distribution. As a result of all five experimental effects, the mean of the P_t-spectrum was increased by 6 MeV/c. The distribution of Φ was measureably affected by the electron energy bias, but all of the other effects caused little change.

Distributions of P_t and Φ for V-A, V and A, for scalar-pseudoscalar, and for tensor are shown (Fig. 13). The P_t-spectrum for V-A is seen to be more easily distinguished from the pure vector than from the pure axial vector P_t-spectrum. It can also be seen that the tensor interaction gives a P_t-distribution similar to that of the V-0.7A interaction.

The V+A interaction (not shown) produces a P_t-spectrum identical to that of the V-A interaction. In principle, the distribution of Φ is affected by changing the relative sign of V and A, but the effect of this change was barely noticeable with samples of 1000 Monte Carlo events. Thus, the V+A interaction was not separately considered.

The similarity of the distributions from different interactions makes it impossible to single out a unique form of the interaction using only 50 experimental events. However, we were able to show that some of the forms are improbable.

E. Study Of Systematic Measurement Error

The procedure of measuring P_t and Φ has been examined for any significant systematic errors. To do this, a random sample of normal Λ decays was selected by criteria similar to those used for the Λ_β decays, i.e. the stopping proton and minimum length requirements. From these events, the distributions of proton transverse-momentum and $\Phi_{p\pi}$ (the angle between the proton and pion in the plane transverse to the Λ direction) were compared to those generated by a Monte Carlo program. This program was a modification of the one used for generating the β-decays. It produced Λ pionic decays and applied the appropriate cutoffs and measurement errors.

There were 544 measured Λ decays after the cutoffs and 1200 Monte Carlo events. The mean value of P_t for the former was 86.7 compared to a mean of 86.2 for the latter, and the X^2 fit of the two P_t distributions (Fig. 14) gave a probability of 30% for obtaining a worse fit. The mean value of $\Phi_{p\pi}$ for the measured sample was 163.1 compared to a mean of 163.4 for the Monte Carlo sample, and the X^2 fit of the two distributions gave a probability of 86% for obtaining a worse fit.

Since the β-decays and the pionic decays were measured in the same way, the close fit of these normal Λ decay distributions to the theoretical distributions demonstrates that there was no detectable bias in the measurement of P_t and Φ.

F. Experimental Results

The distributions of P_t and Φ for the 50 R_{max} events are shown in Fig. 15 and Fig. 16. These histograms were compared with the theoretical distributions of P_t and Φ by calculating the χ^2 probabilities for each distribution using 3 degrees of freedom. The values of χ^2, along with their percentiles, are given in Table II.

Fig. 17 shows the curve of the likelihood ratios for the different interactions with respect to pure vector. The best fit to the P_t data is given by pure axial vector and, about equally, by pure scalar. The Φ data, on the other hand, favor an equal mixture of V and A. However, the generally greater likelihood ratios for the P_t curve indicates that P_t is more sensitive to the form of the interaction than is Φ. The mean values of P_t and Φ from the data are also compared to the various theoretical values in Table II. Again, P_t, with a mean value of 86 ± 6 MeV/c, favors scalar and Φ, with a mean value of 128° ±7°, favors V-A.

To obtain the combined result from P_t and Φ and to show that the separate results are not incompatible, the fifty R_{max} events were plotted on a scatter diagram (Fig. 18) with Φ along the ordinate and P_t along the abscissa. With the two variables thus correlated one can determine the most probable form of the interaction and also determine whether the configuration of points on the scatter diagram is a likely result from such an interaction.

The problem was simplified by dividing the scatter diagram into 25 equal boxes, each 40 MeV/c by 36°. Similarly, the theoretical distributions became two dimensional histograms. For a given form of the interaction each event has a probability g_i of falling into box i. If N_1 events fall into box 1, N_2 events into box 2, etc., the likelihood for a particular experimental result, N_1, N_2. . . N_{25}, is given by:

$$\mathcal{L} = \prod_{i=1}^{25} g_i^{Ni} , \qquad \text{where} \sum_{i=1}^{25} g_i = 1.$$

The g_i's were determined for nine different forms of the decay interaction: V, V-1/3A, V-2/3A, V-A, V-3/2A, V-3A, A, scalar, and tensor. To do this, approximately 20 000 Monte Carlo events were generated from each interaction and plotted on the scatter diagrams. The number of events falling in each box was divided by the total number to obtain the normalized g_i's.

The likelihood of the experimental result was calculated for each of the nine interactions relative to pure vector. In Fig. 19 a continuous curve is drawn through these values from V through A, and values for scalar and tensor are also shown. The ratio of the ordinates of any two points gives the relative likelihood of the two corresponding interactions.

The curve rises sharply in going from vector to V-A; it then levels off in going from V-A to axial vector. The likelihood ratio between V-A and pure vector favors V-A by $\sim 10^5$ to one. Between V-A and pure axial vector the ratio is only two to one in favor of axial vector. Scalar has the same likelihood as pure axial vector, but tensor is lower by a factor of 40.

It is interesting to see how the statistical fluctuations associated with 50 events are reflected in the likelihood curves.

To show this, 200 Monte Carlo "experiments" of 50 events each were run for three interactions: A, V-A, and V-0.33A, and their likelihood curves were calculated. Five typical curves for each interaction are shown in Figs. 20 through 22; the top and bottom curves are the extremes and the dotted curve is the average for each group of 200. These dotted curves show the average sensitivity of 50 events for distinguishing the interaction and they indicate the expected shape for a likelihood curve. The other curves show the type of variation that can be expected.

The shapes of the likelihood curves for V-A and A are similar to each other but different from those for V-0.33A. The curve of the actual experiment fits consistently into either the axial vector set or the V-A set, although the likelihood ratio between A and V is larger than the expected value. This ratio is one standard deviation higher than that expected from a pure axial vector interaction and two standard deviations higher than that expected from a V-A interaction. It is higher than the expected A/V likelihood ratio from a V-0.33A interaction by three standard deviations. This indicates that our experimental result is not improbable for the more likely interactions V-A and A. It also indicates that the V-0.33A interaction is unlikely.

The chi-square method was used to determine the absolute goodness of fit of the data to the several theoretical distributions. For this, each of the two-dimensional plots of P_t vs. Φ was divided into four areas containing approximately the same number of events and the total number was normalized to 50.

The values of χ^2 and the corresponding percentiles are given in Table IV. Pure tensor is ruled out with 99% confidence. Further, if the interaction is confined to mixtures of V and A, the results rule out mixtures with $|C_A|/|C_V| < 0.5$ with 99% confidence.

V. CONCLUSION

The three determinations of the branching ratio are shown below:

(a) Branching Ratio from R_{max} = $(0.82 \pm 0.13) \times 10^{-3}$

(b) Branching Ratio from δ rays = $(0.70 \pm 0.31) \times 10^{-3}$

(c) Branching Ratio from kinematics = $(0.62 \pm 0.22) \times 10^{-3}$

Events used to determine (a) are separate from those used to determine (b) and (c). Although the three methods sample different parts of the electron energy spectrum, all three values agree within the errors. The confirmation of the branching ratio from R_{max} by the δ ray and kinematic methods, in spite of much larger uncertainties, is valuable since the only common link in determining the ratios is the Monte Carlo Calculation of detection efficiencies.

The R_{max} events provide the best value for the branching ratio. The 15% error quoted contains both the statistical uncertainty and the errors on the scanning efficiencies. Formerly the best estimate of the ratio was that of Aubert et al.,[4] who found $(3.0^{+1.5}_{-1.2}) \times 10^{-3}$. The value found in the present work is clearly in disagreement with the prediction of 16×10^{-3} made by Feynman and Gell-Mann.[1]

In the study of the form of the interaction, the "induced" form factors have been neglected. The χ^2 probabilities show that the pure tensor interaction can be ruled out with 99% confidence. If the interaction is V and A only, then the ratio $|x| = |C_A|/|C_V|$ >0.5 with 99% confidence. The interactions scalar, V-A, and pure axial vector are consistent with the data.

This result is compatible with the result of Baglin et al. and with the prediction of Cabibbo's theory. It is incompatible with theories that predict a predominantly vector interaction, such as the theory of Cornwall and Singh.

ACKNOWLEDGEMENTS

During my tenure as a graduate student I have received guidance and encouragement from many people. First, I would like to thank Professor Wilson M. Powell, who has been my research advisor, for introducing me to high energy physics and for providing the present topic for my research project.

The determination of the branching ratio, reported in the first part of this paper, was done by several individuals. Those from the Lawrence Radiation Laboratory were Dr. Robert Ely, Dr. George Gidal, Dr. George Kalmus, and Professor Wilson Powell. Those from University College London were Dr. Frederick Bullock, Dr. Cyril Henderson, Mr. David Miller, and Dr. F. Russell Stannard.

I would like to give special thanks to Dr. Robert Ely and Dr. George Gidal for their willing guidance during my graduate years, and to Dr. Cyril Henderson and Dr. George Kalmus for their aid and advice.

Mr. Paul Weber was in charge of measuring and did a great deal to organize the processing of data. Major parts of the scanning were done by Mr. Steve Bates, Mrs. Rho Gamow, Miss Bernadette Requiro, Mr. Robert Williams, and Mrs. Toni Woodford.

I am indebted to Howard White and his co-workers for data-reduction programs, and to Mr. Gary Griffin, Mr. Larry Oswald, and Mr. Frank Swartz for their work on the chamber.

I am grateful to Mrs. Marleigh Sheaff for doing many calculations and to Miss Kathy Tennant for typing this manuscript.

Finally, to my fellow graduate students I offer my sincere thanks for their unselfish assistance.

APPENDIX

The present experiment has been confined to measuring the distributions P_t and Φ, defined in Fig. 6, using only 50 events. The likelihood curve in Fig. 21a shows the expected result for an experiment involving 50 Λ_β decays assuming the interaction is V-A. This curve indicates that on the average it is difficult to distinguish V-A from pure A with 50 events.

In Fig. 23 the expected likelihood functions for results of 100, 200, 300, 400, and 500 events are plotted, assuming a V-A interaction. Even with 500 events, the average likelihood ratio is only about 200 to one between V-A and A, and less between any two intermediate mixtures of V and A.

The conclusion is that using the present method a sharp determination of the form of the interaction can hardly be achieved even by increasing the number of events by an order of magnitude.

REFERENCES

1. R. P. Feynman and M. Gell-Mann, Phys. Rev. 109, 193 (1958).

2. E. C. G. Sudarshan and R. E. Marshak, Phys. Rev. 109, 1860 (1958).

3. W. E. Humphrey, J. Kirz, A. H. Rosenfeld, J. Leitner, and Y. I. Rhee, Phys. Rev. Letters 6, 478 (1961).

4. B. Aubert, V. Brisson, J. Hennessy, P. Mittner, J. Six, C. Baglin, M. Bloch, A. Bressy, A. Lagarrigue, A. Orkin-Lecourtois, P. Rancon, A. Rousset, and X. Sauteron, in Proceedings of the Aix-en-Provence International Conference, Vol. 1, p. 197 (1961).

5. R. P. Ely, G. Gidal, G. E. Kalmus, L. O. Oswald, W. M. Powell, W. J. Singleton, F. W. Bullock, C. Henderson, D. J. Miller, and F. R. Stannard, Phys. Rev. 131, 868 (1963).

6. N. Cabibbo, Phys. Rev. Letters 10, 531 (1963).

7. J. J. Sakurai, Phys. Rev. Letters 12, 79 (1964).

8. J. M. Cornwall and V. Singh, Phys. Rev. Letters 10, 551 (1963).

9. C. Baglin, V. Brisson, A. Rousset, J. Six, H. H. Bingham, M. Nikolic, K. Schultze, R. T. Elliott, L. K. Rangan, A. Haatuft, and K. Myklebost, Phys. Rev. Letters 6, 186 (1963).

10. W. M. Powell, W. B. Fowler, and L. O. Oswald, Rev. Sci. Instr. 29, 874 (1958).

11. P. Bastien, O. Dahl, J. Murray, M. Watson, R. G. Ammar, and P. Schlein, in Proceedings of an International Conference on Instrumentation for High-Energy Physics, Lawrence Radiation Laboratory, University of California at Berkeley, September 1960 (Interscience Publishers, Inc., New York, 1961).

12. Reference Manuals. FOG-CLOUDY-FAIR Bubble Chamber Processing System. Lawrence Radiation Laboratory Document UCID 1340 (unpublished).

13. F. S. Crawford, in Proceedings of the 1962 International Conference on High-Energy Physics (CERN, Geneva, 1962), p. 832.

14. D. J. Miller, University College London Bubble Chamber Group Report Number DJM/01, 1962 (unpublished).

15. R. Sternheimer, Phys. Rev. 88, 851 (1952).

16. W. Heitler, The Quantum Theory of Radiation (Oxford University Press, Amen House, London, 1957), 3rd Ed., p. 378.

17. H. W. Koch and J. W. Motz, Rev. Mod. Phys. 31, 920 (1959).

18. W. H. Barkas and A. H. Rosenfeld, University of California Radiation Laboratory Report UCRL-8030, 1961 (unpublished).

19. L. Egardt, Nuovo Cimento 27, 357 (1963).

20. D. R. Harrington, Phys. Rev. 120, 1482 (1960).

Table I. Numbers of events and branching ratios.

Category	No. observed	Scanning efficiency (%)	Estimated background (% observed)	Cutoff correction (%)	Detection efficiency (%)	Total	Branching ratio
Mesonic decay	192,000	89±1	<2	0	100±2	322,000±10,000	
R_{max} 30°≤dip angle≥-30°	62	87±5	<3	90±3[a] 50±0[b]	60±2	264±40	$(0.82\pm0.13)\times10^{-3}$
Delta rays*	12	67±15	17	94±2[c]	7.1±1.5	224±100	$(0.70\pm0.33)\times10^{-3}$
Kinematic events	17	90±7	10	47±4[d]	18±4	200±80	$(0.62\pm0.25)\times10^{-3}$

*Events are not included in these categories if they satisfy the R_{max} condition.

[a] $\ell_p \geq 2$ mm and $\ell_e \geq 9$ cm

[b] Dip angle between ±30°

[c] $\ell_p \geq 2$ mm

[d] Above line in Fig. 3

Table II. χ^2 probabilities for different forms of the interaction; from P_t and Φ data separately.

Form of interaction	Vector	V-.33A	V-.67A	V-A	V-1.5A	V-3A	Axial Vector	Scalar	Tensor
χ^2 of P_t distributions	26.7	16.7	8.5	5.4	3.8	2.8	2.3	0.2	10.1
Percentile from P_t	<<1%	<1%	4%	15%	28%	43%	50%	98%	2%
χ^2 of Φ distributions	4.3	3.0	0.25	0.07	0.24	0.54	0.75	4.29	0.25
Percentile from Φ	23%	39%	97%	>99%	97%	91%	86%	23%	97%

Table III. Mean values of theoretical distributions of P_t and Φ.

Form of interaction	V	V-.33A	V-.67A	V-A	V-1.5A	V-3A	Axial Vector	Scalar	Tensor
Mean value of P_t (MeV/c) from modified theoretical distributions	112	108	102	99	97	95	93	85	103
Mean P_t from experiment	---	---	---	---	---	---	---	→ 86±6	
Mean value of Φ (deg.) from modified theoretical distributions	141	137	132	128	126	124	123	116	132
Mean Φ from experiment	---	---	---	→ 128±7					

Table IV. χ^2 percentiles for combined distributions of P_t and Φ.

Form of interaction	V	V-.33A	V-.67A	V-A	V-1.5A	V-3A	A	Scalar	Tensor
Value of χ^2	27.0	17.1	9.1	6.7	5.3	4.6	4.2	3.8	11.0
Percentile	<<1%	<<1%	3%	8%	15%	21%	24%	28%	1%

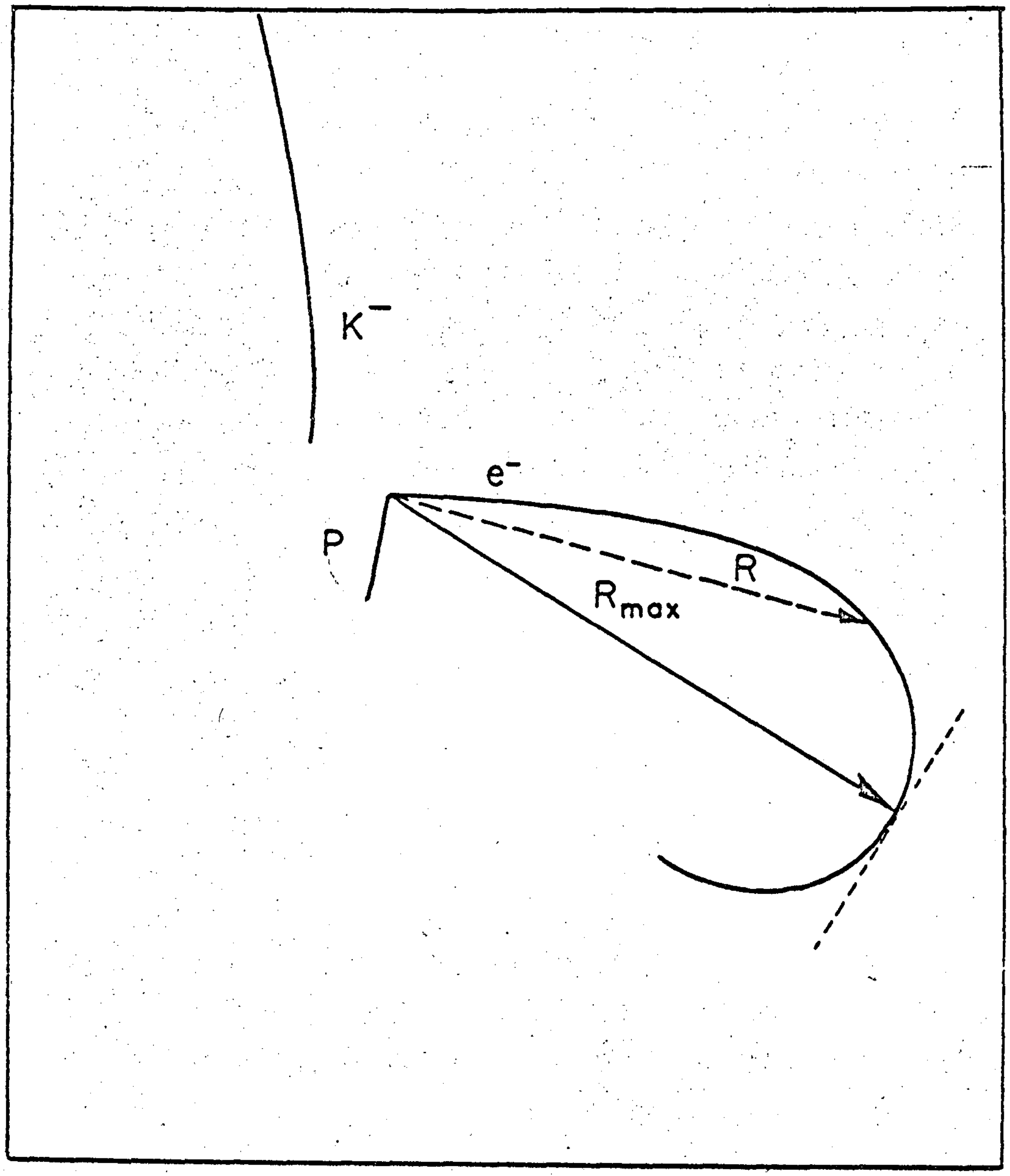

MUB-2727

Fig. 1 Example of an R_{max} event. The radius vector R from the point of decay to a point on the electron track passes through a maximum value.

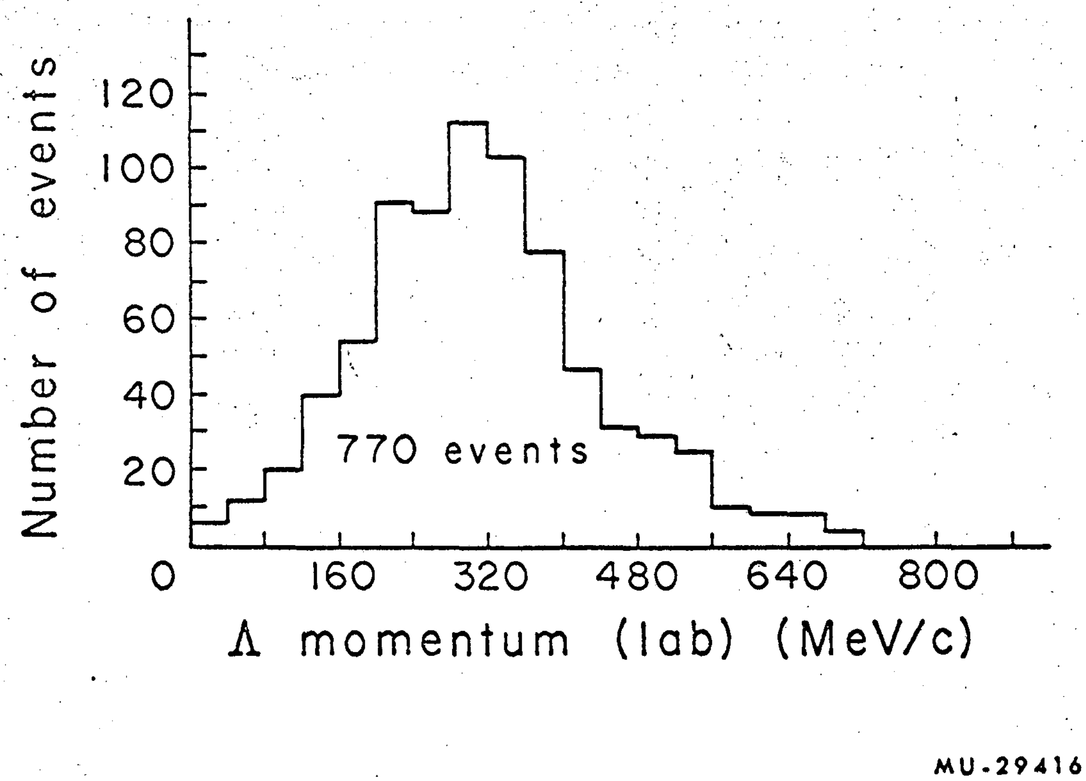

Fig. 2 Histogram of Λ momentum in the laboratory system.

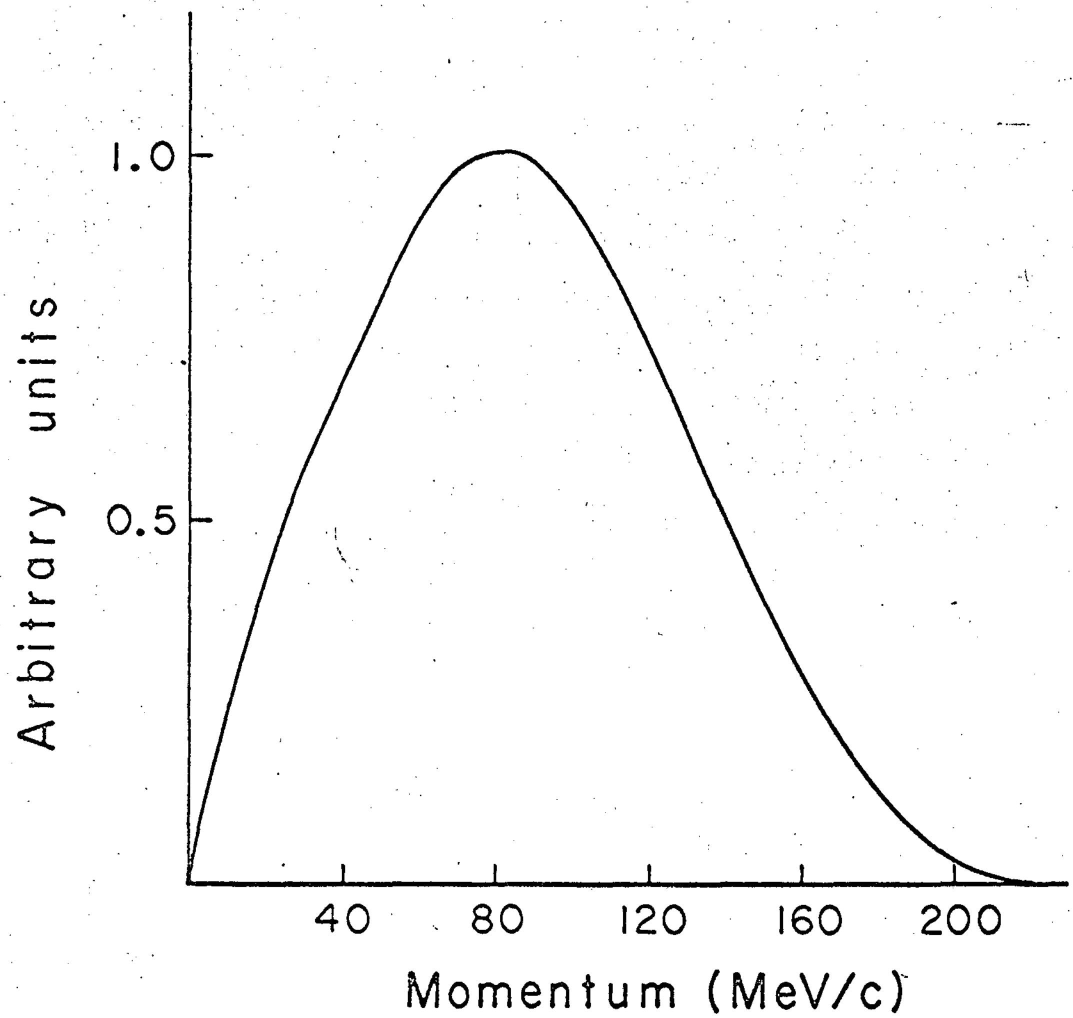

Fig. 3 Laboratory-system electron-momentum spectrum obtained by folding the Λ-momentum distribution (Fig. 2) into a three-body Lorentz-invariant phase-space calculation.

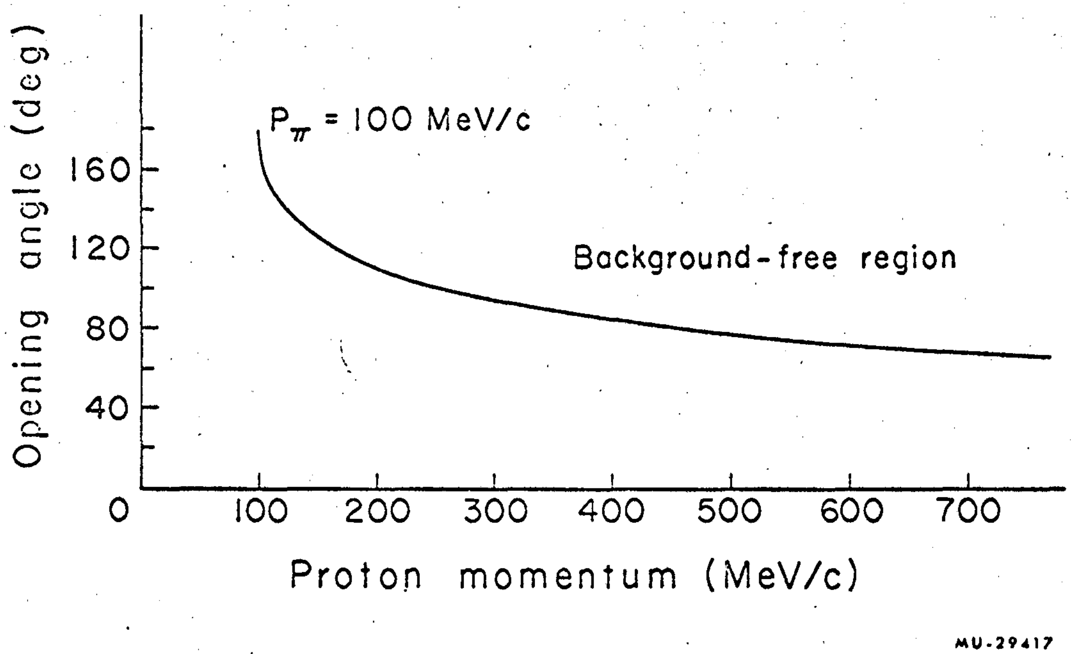

Fig. 4 Opening angle between charged tracks vs. proton momentum. Background from mesonic Λ decays falls below line.

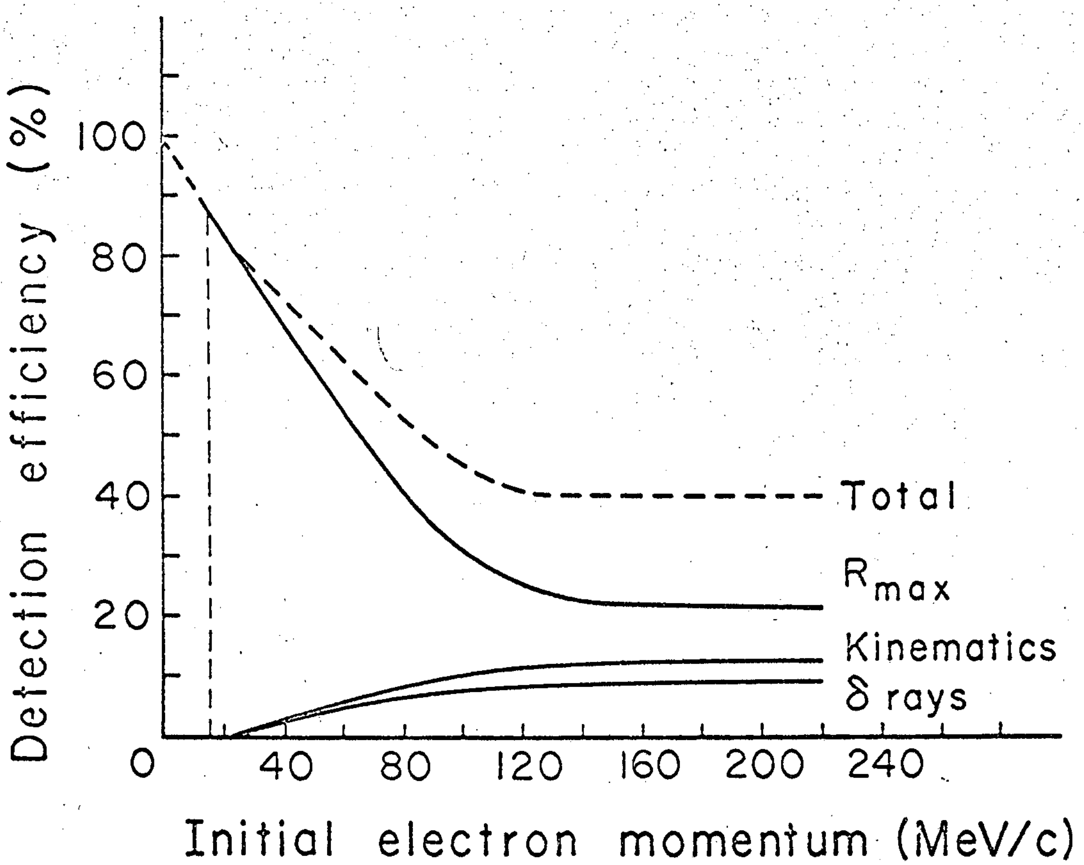

Fig. 5 Electron-detection efficiency curves for the three methods of identification. Dashed vertical line defines a 9-cm cutoff used for R_{max} events. Total curve is slightly lower than the sum of the other three curves due to a 10% overlap of kinematic and δ ray events. A 100% scanning efficiency is assumed for all curves.

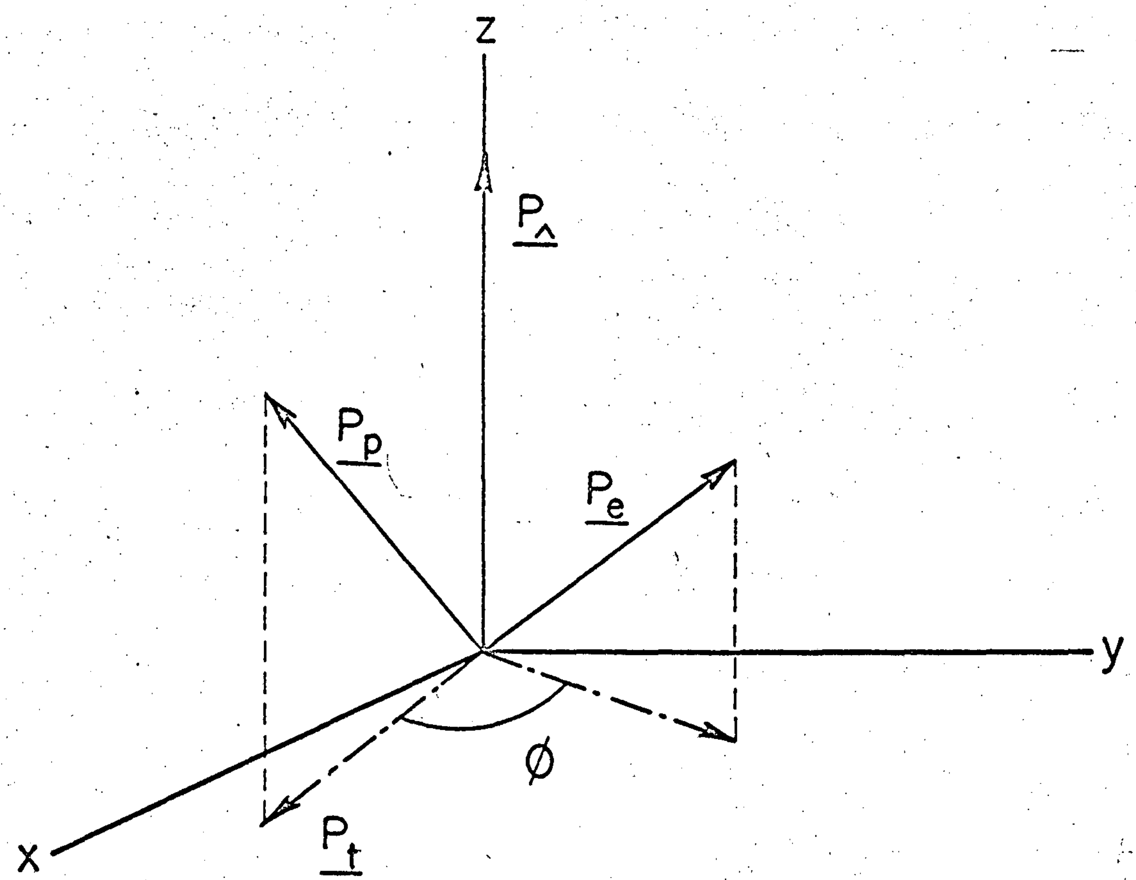

MUB-2723

Fig. 6 Proton transverse momentum and angle Φ between proton and electron in Λ transverse plane. Λ is shown traveling along positive Z axis before decay. The x,y plane corresponds to the Λ transverse plane.

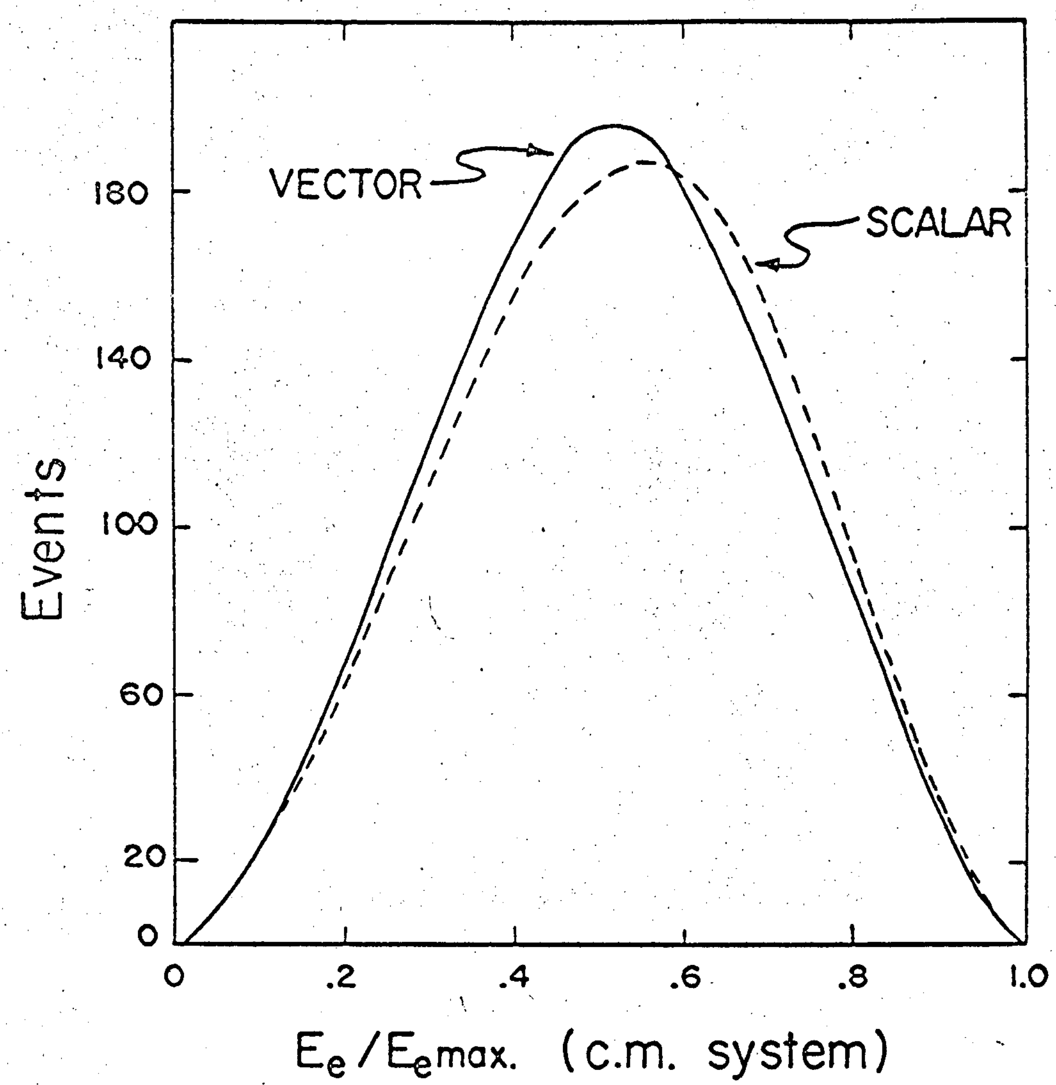

MUB-2729

Fig. 7 Electron energy spectrum in C.M. system for vector and scalar interactions. Energy spectra for other forms of the interaction are intermediate.

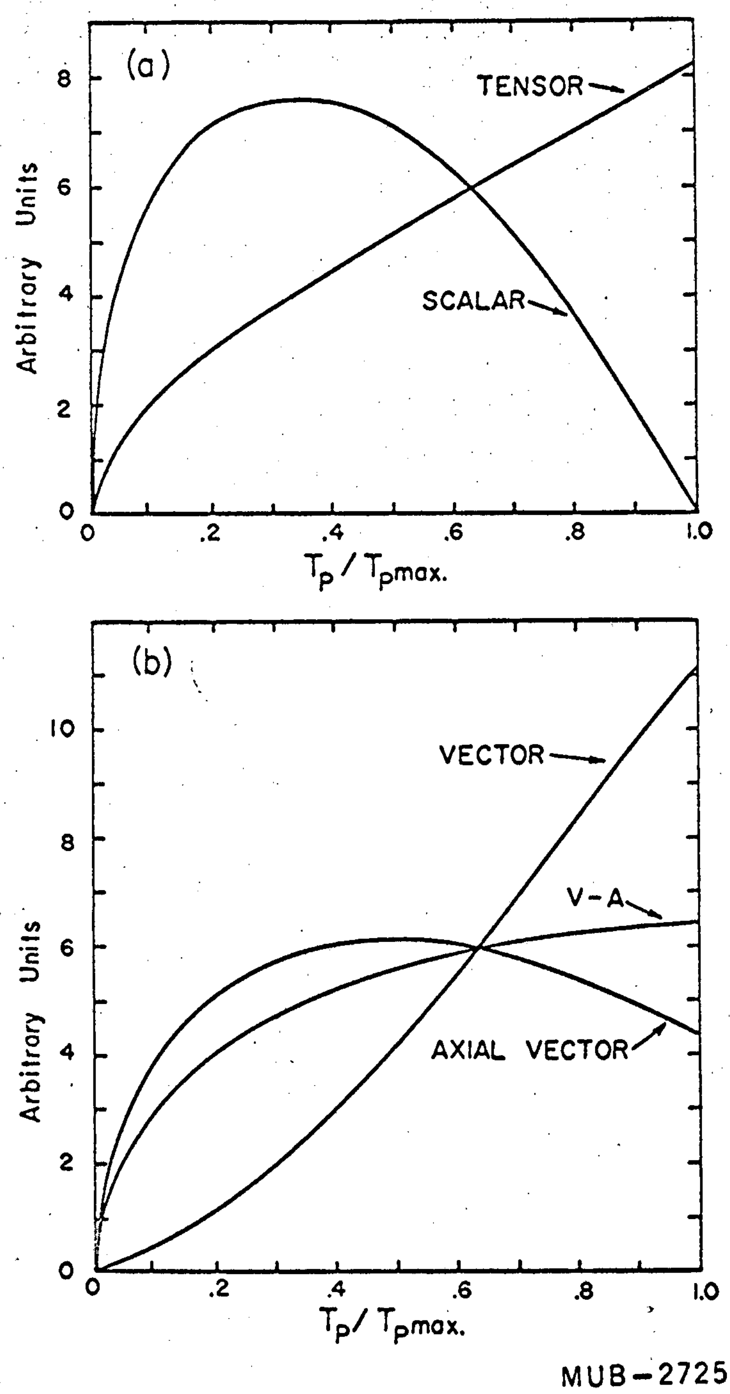

Fig. 8 Proton kinetic energy spectra in C.M. system of Λ_β decay arising from (a) tensor and scalar; (b) vector, V-A, and axial vector interactions.

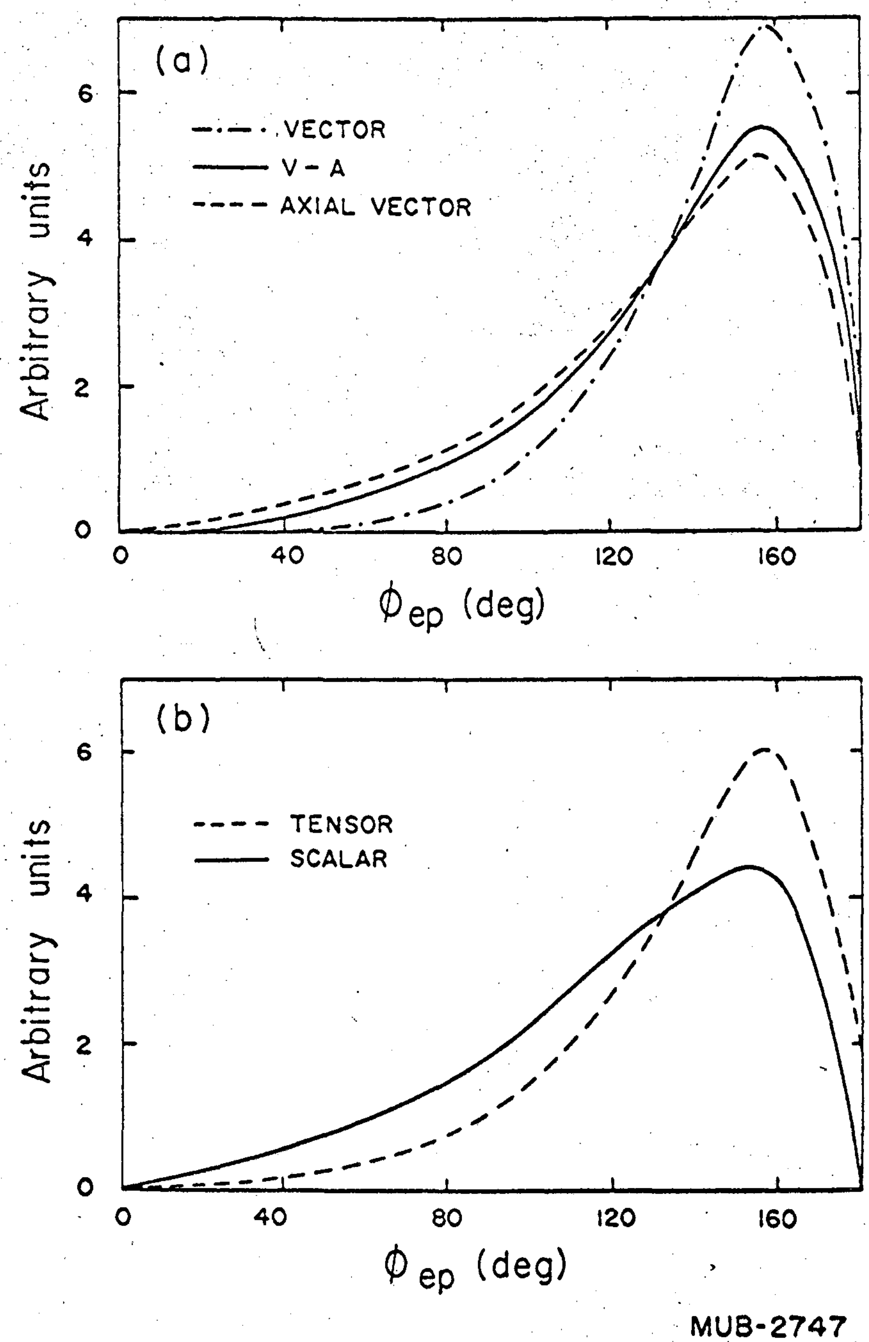

Fig. 9 C.M. distributions of angle Φ_{ep}, between proton and electron momenta, for five different forms of the interaction.

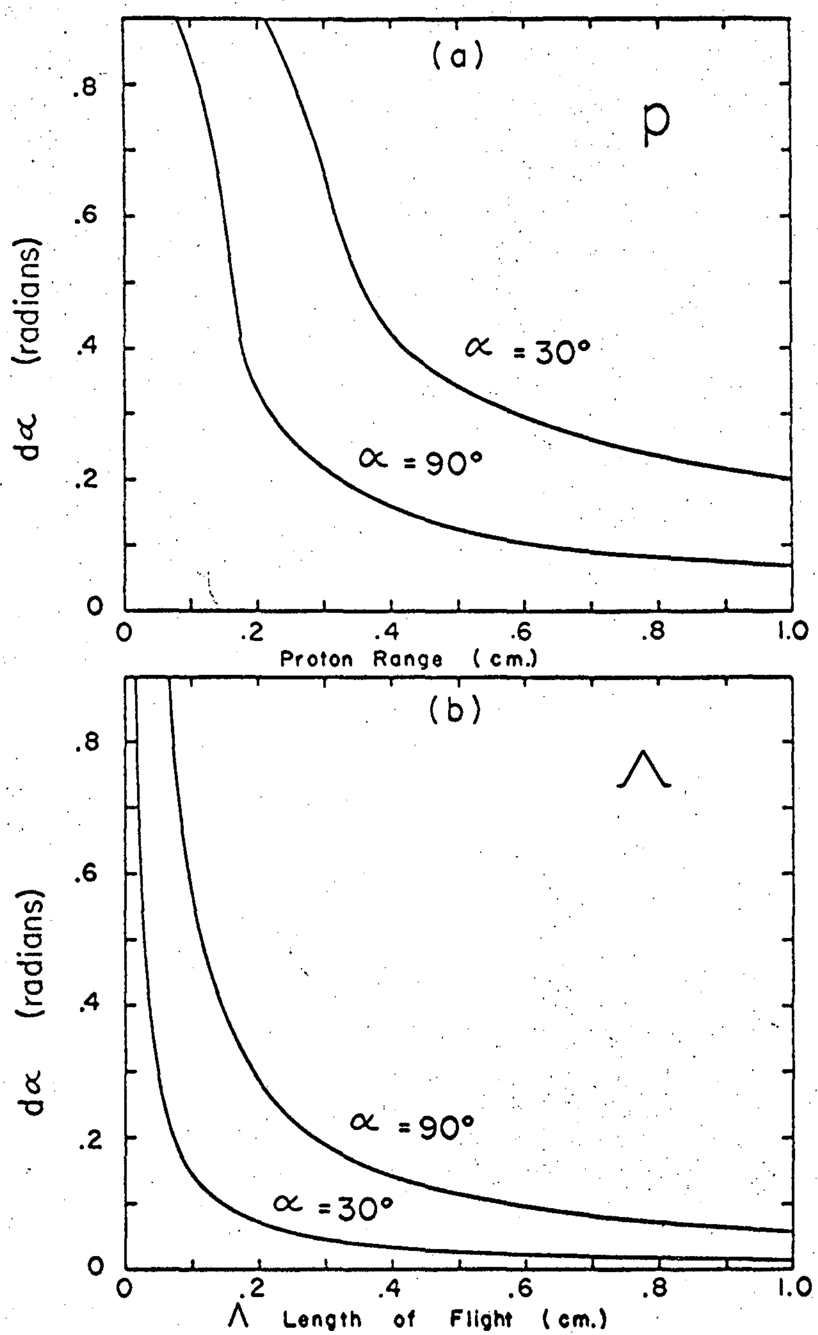

MUB-2733

Fig. 10 Mean error in dip angle α for (a) proton tracks as a function of range, and (b) Λ line-of-flight as a function of length. α is measured from the vertical axis in the chamber.

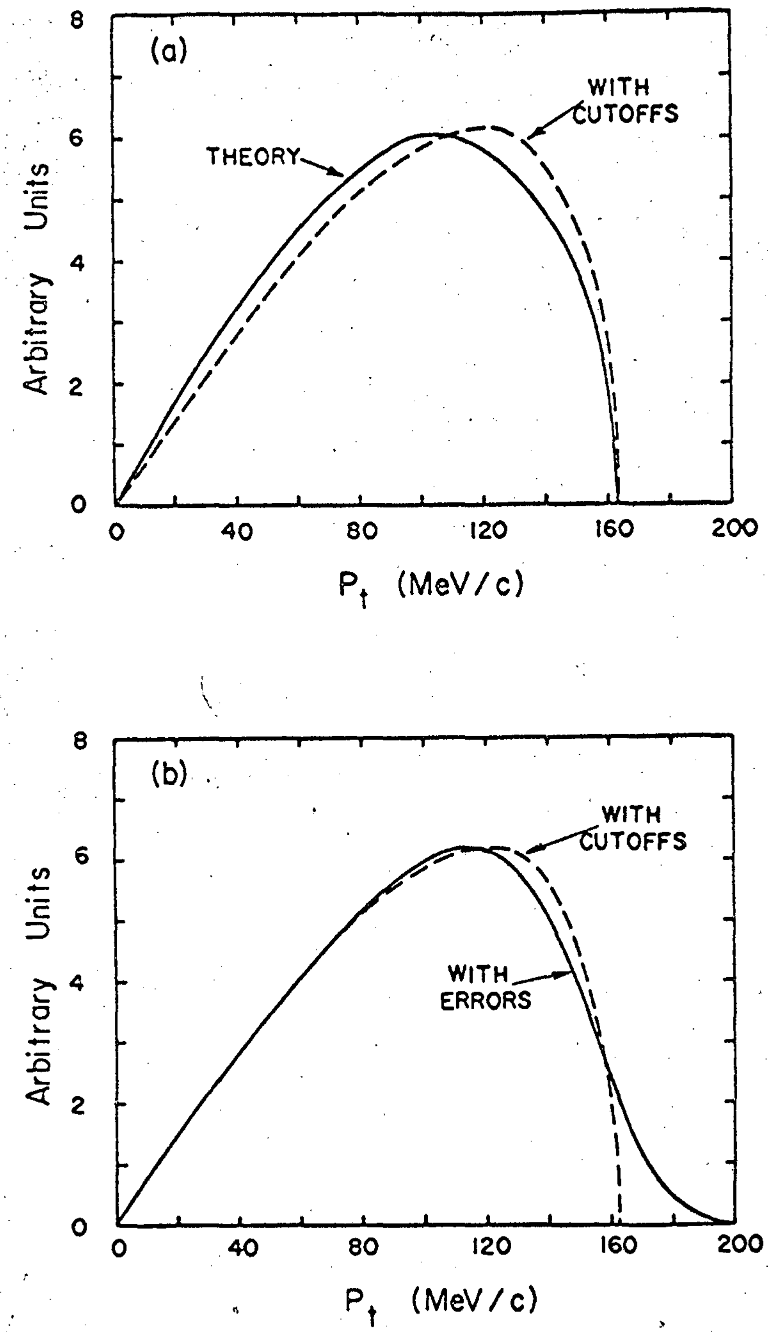

MUB-2724

Fig. 11 (a, b) Proton transverse momentum (P_t) distribution from Λ_β decay with V-A interaction. In (a) are shown the pure theoretical distribution and that remaining after applying proton and Λ length cutoffs and chamber volume effects. In (b) are shown the same curve as above and that resulting after applying multiple scattering and measurement errors.

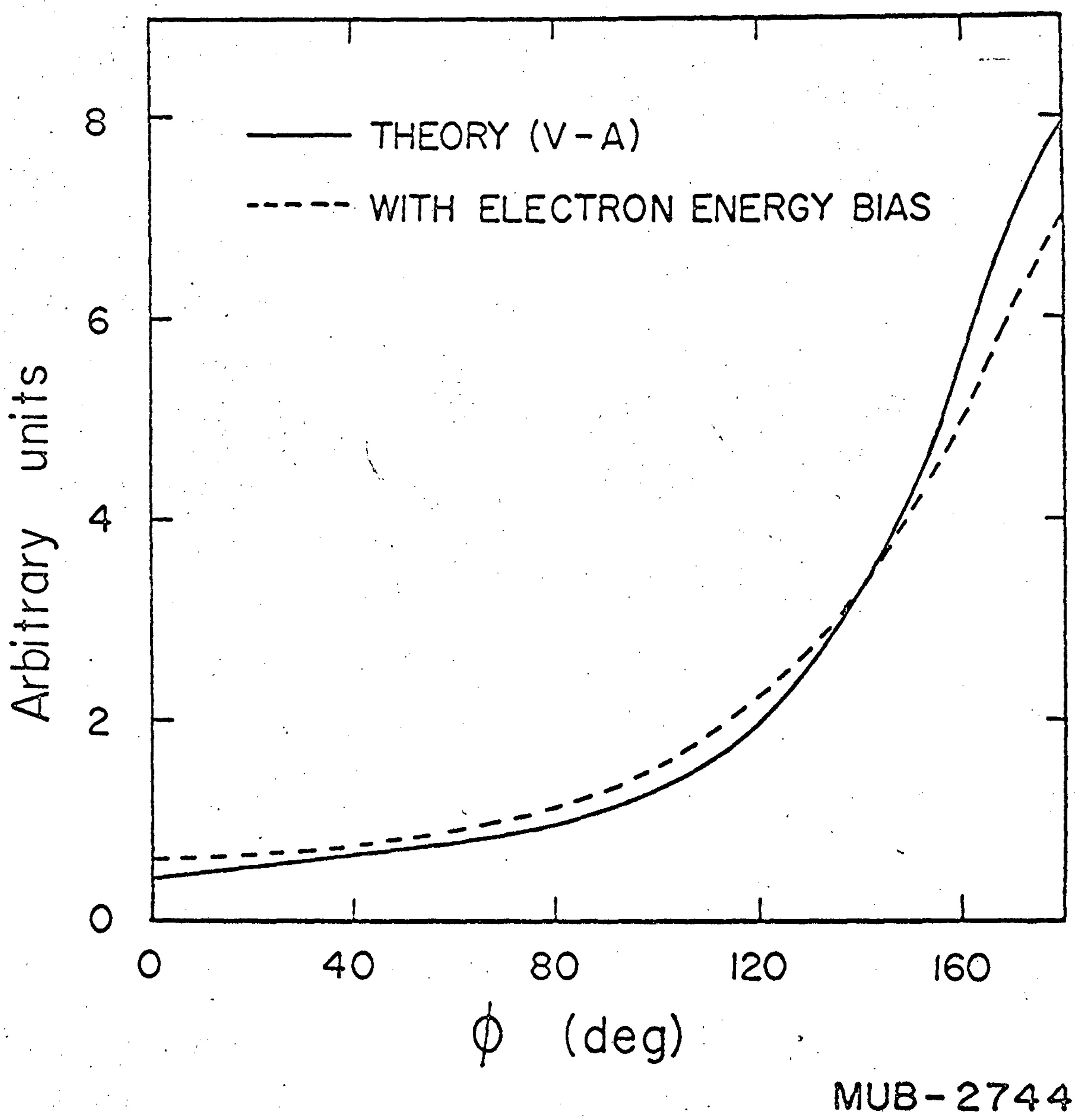

Fig. 12 Distribution of angle between proton and electron projected on Λ transverse plane. Solid line is theoretical V-A curve. Broken line shows distribution after folding in electron energy bias (Fig. 5). Other experimental effects do not alter the distribution.

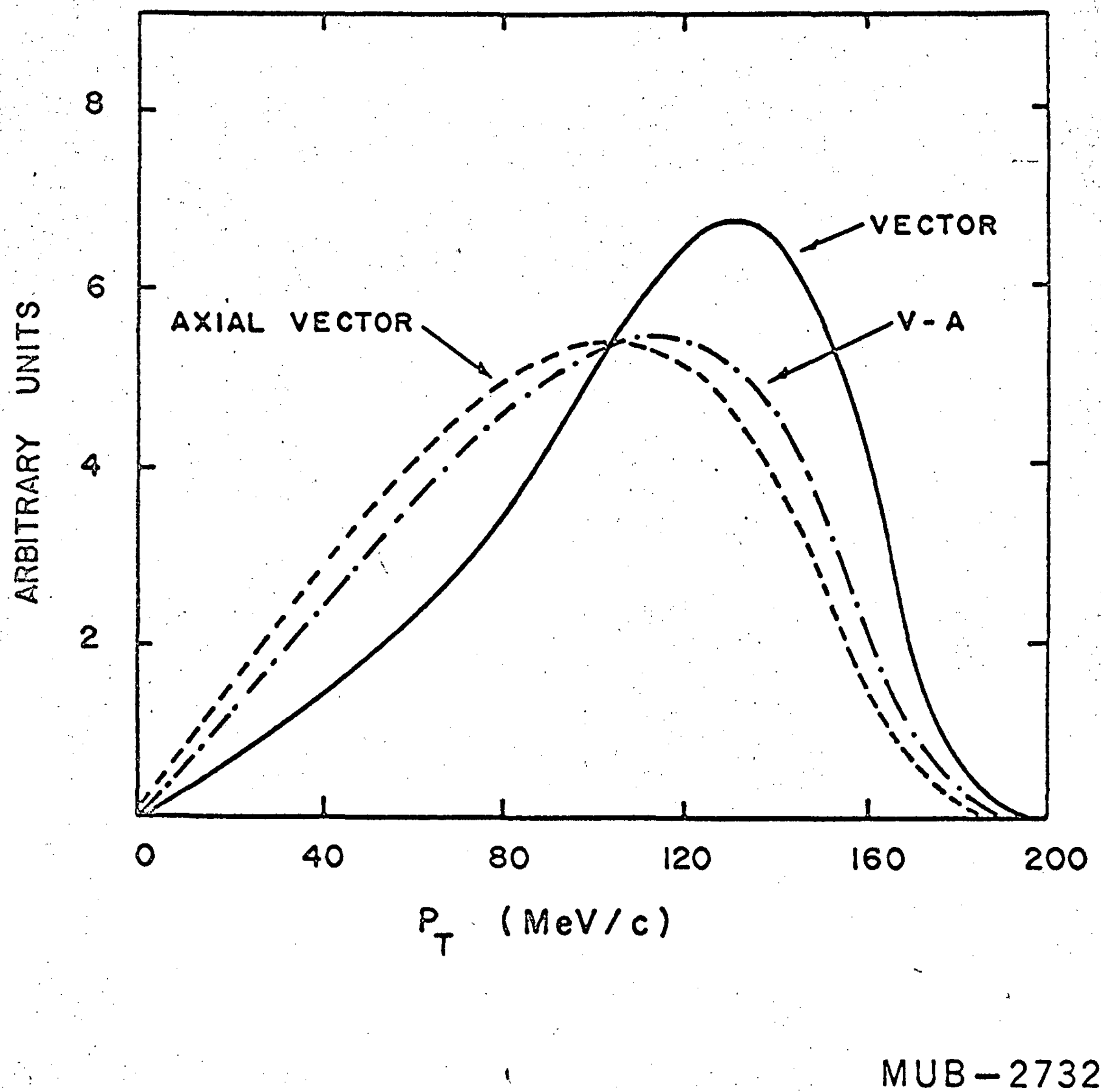

Fig. 13a Proton transverse momentum spectrum with experimental effects folded in; vector, V-A, and axial vector interactions.

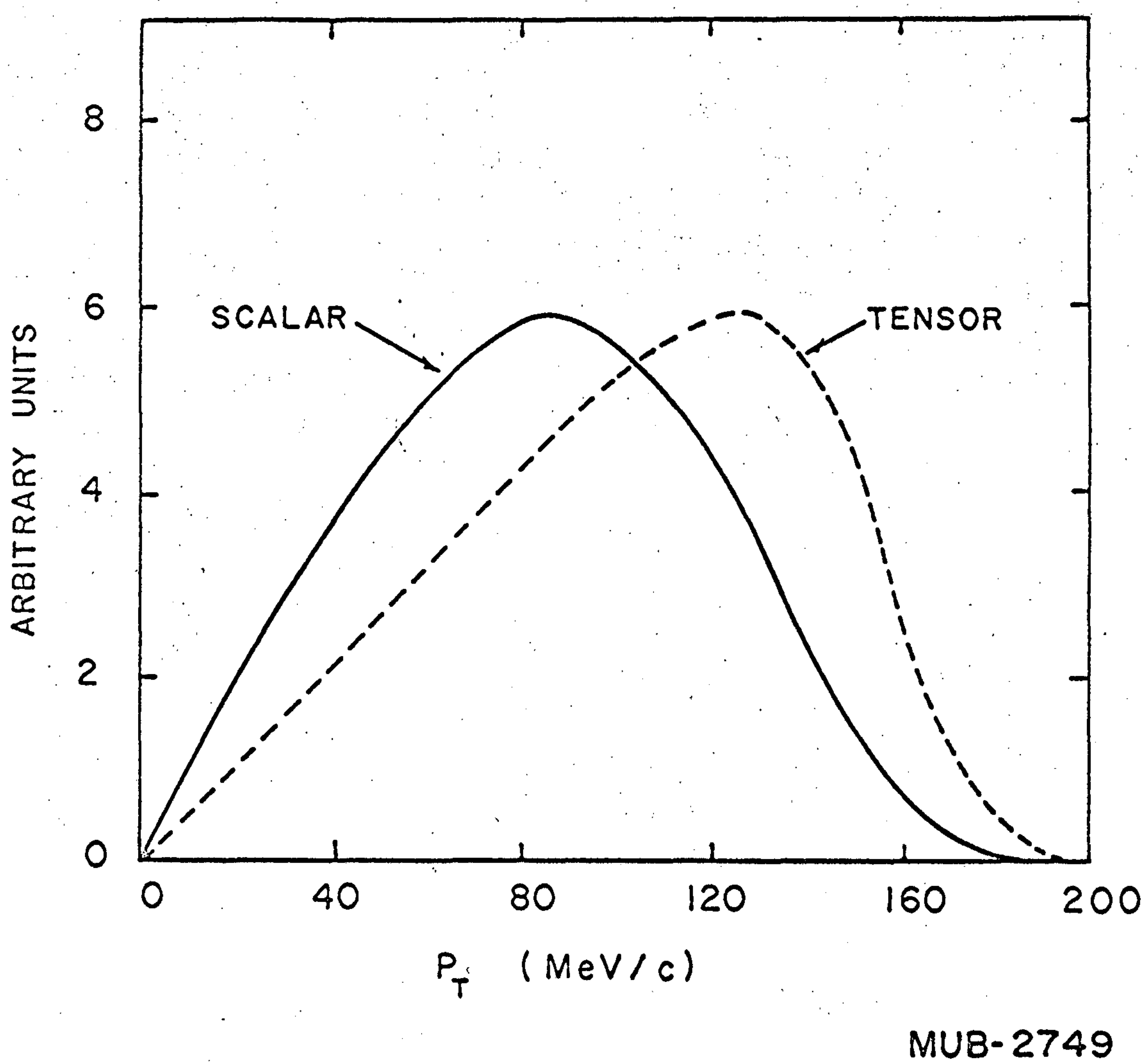

Fig. 13b Proton transverse momentum spectrum with experimental effects folded in; scalar and tensor interactions.

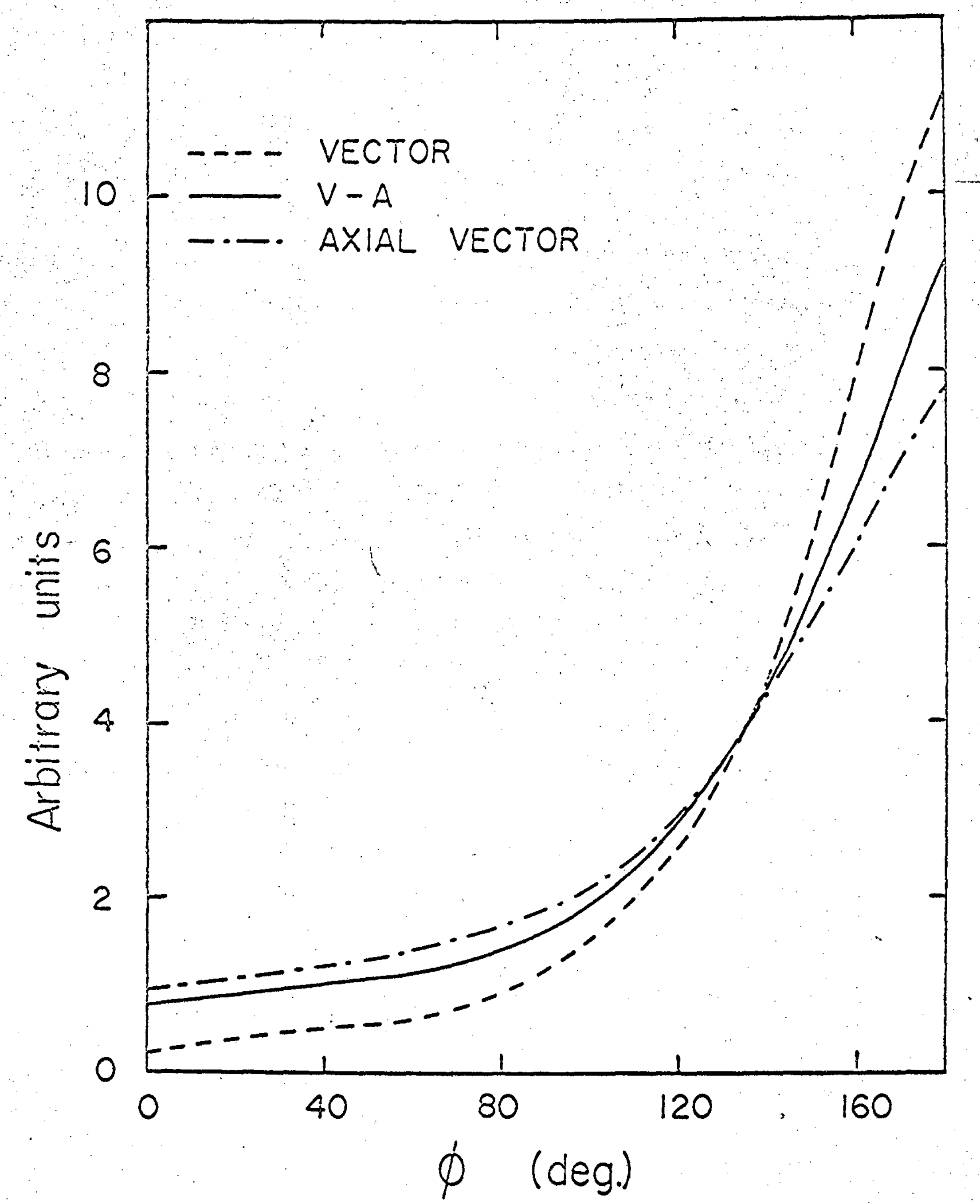

MUB-2722

Fig. 13c Distribution of angle between proton and electron projected on Λ transverse plane; vector, V-A, and axial vector interactions.

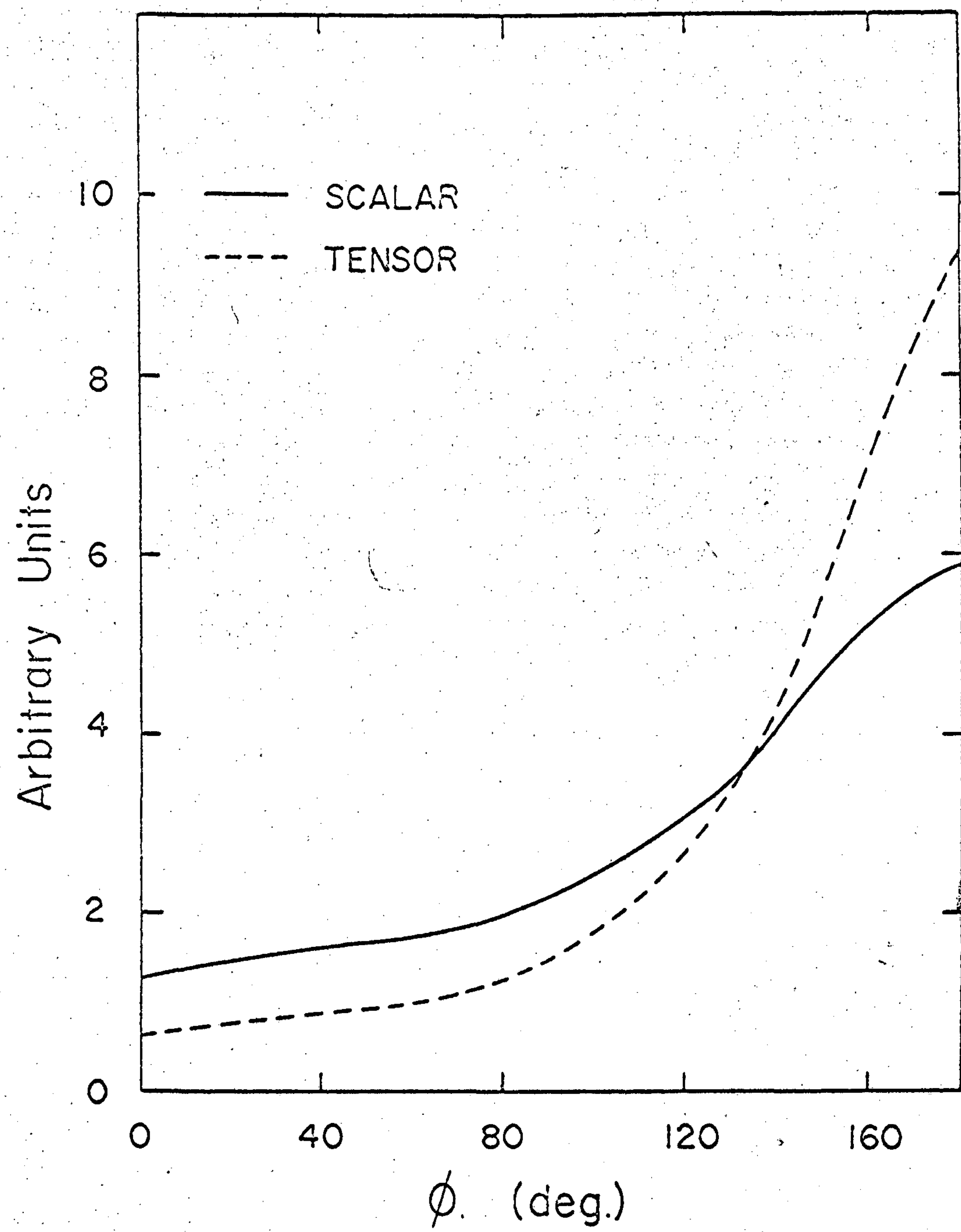

MUB-2721

Fig. 13d Distribution of angle between proton and electron projected on Λ transverse plane; scalar and tensor interactions.

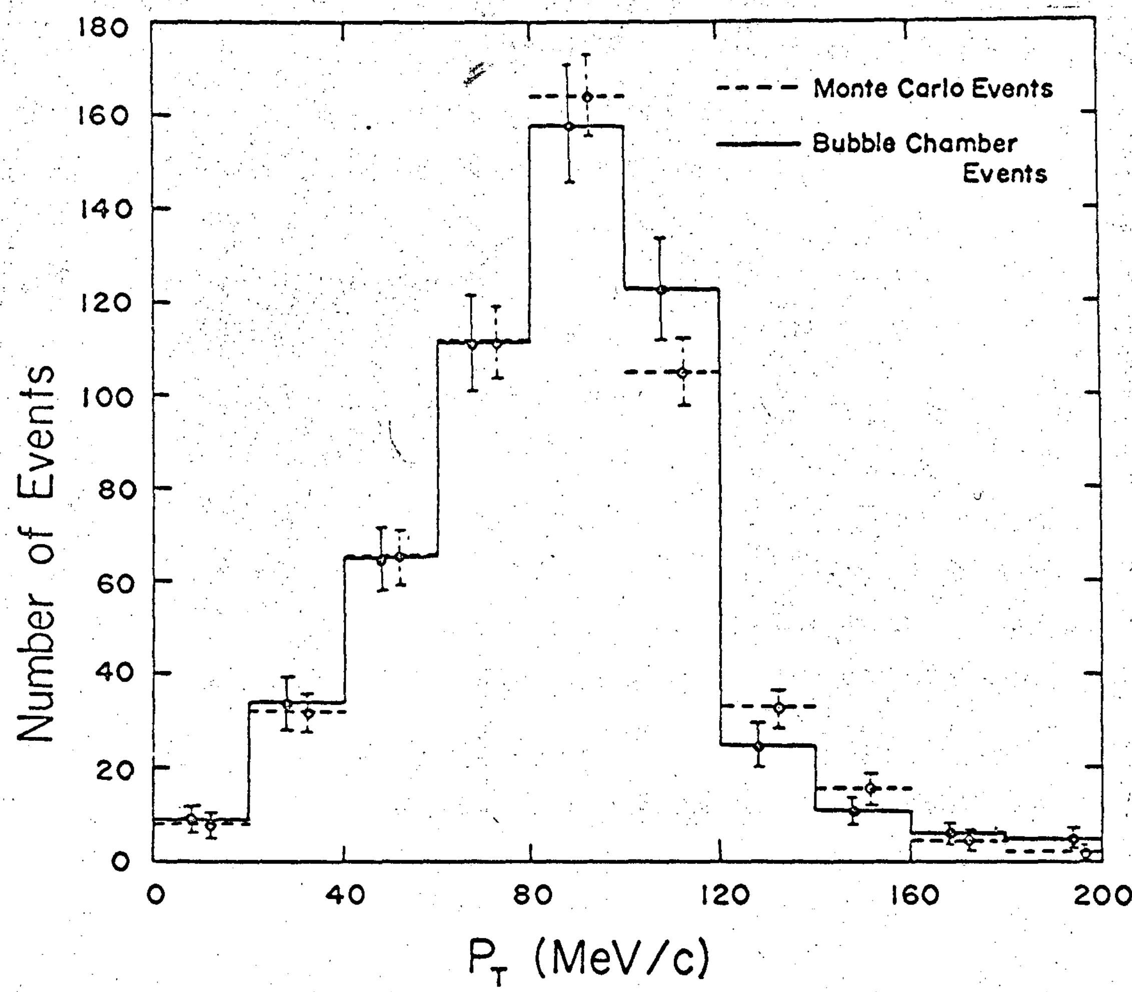

MUB-2728

Fig. 14a Solid line is transverse momentum distribution; a sample of 544 $\Lambda \rightarrow p + \pi^-$ decays found in bubble chamber. Broken line is P_t-distribution of 1200 Monte Carlo events normalized to 544.

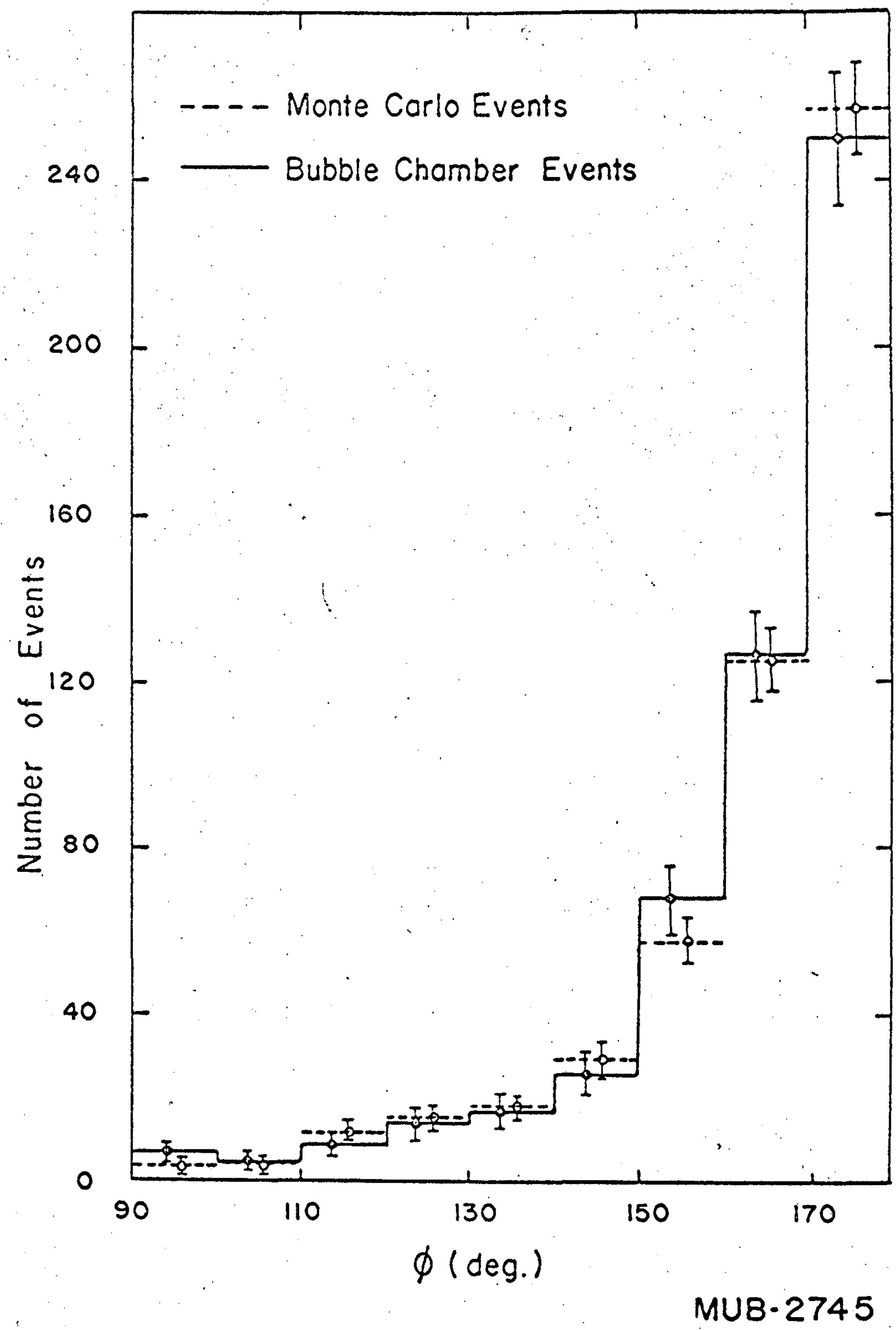

Fig. 14b Solid line is distribution of the projected angle between proton and pion on Λ transverse plane for sample of 544 $\Lambda \rightarrow p + \pi^-$ decays found in bubble chamber. Broken line represents 1200 Monte Carlo events.

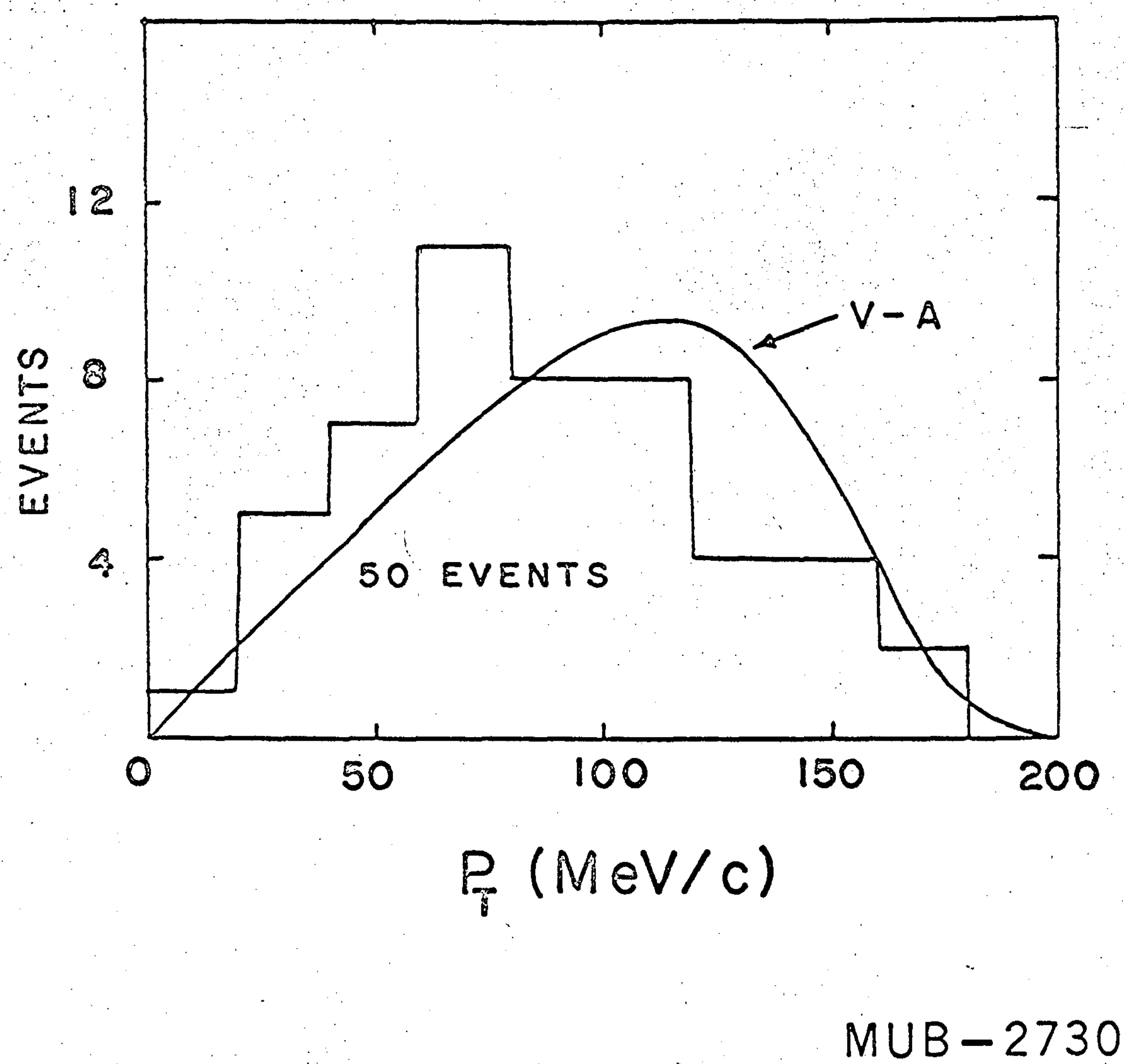

Fig. 15 Proton transverse momentum for 50 R_{max} Λ_β decays. V-A curve with experimental effects folded in, shown for comparison.

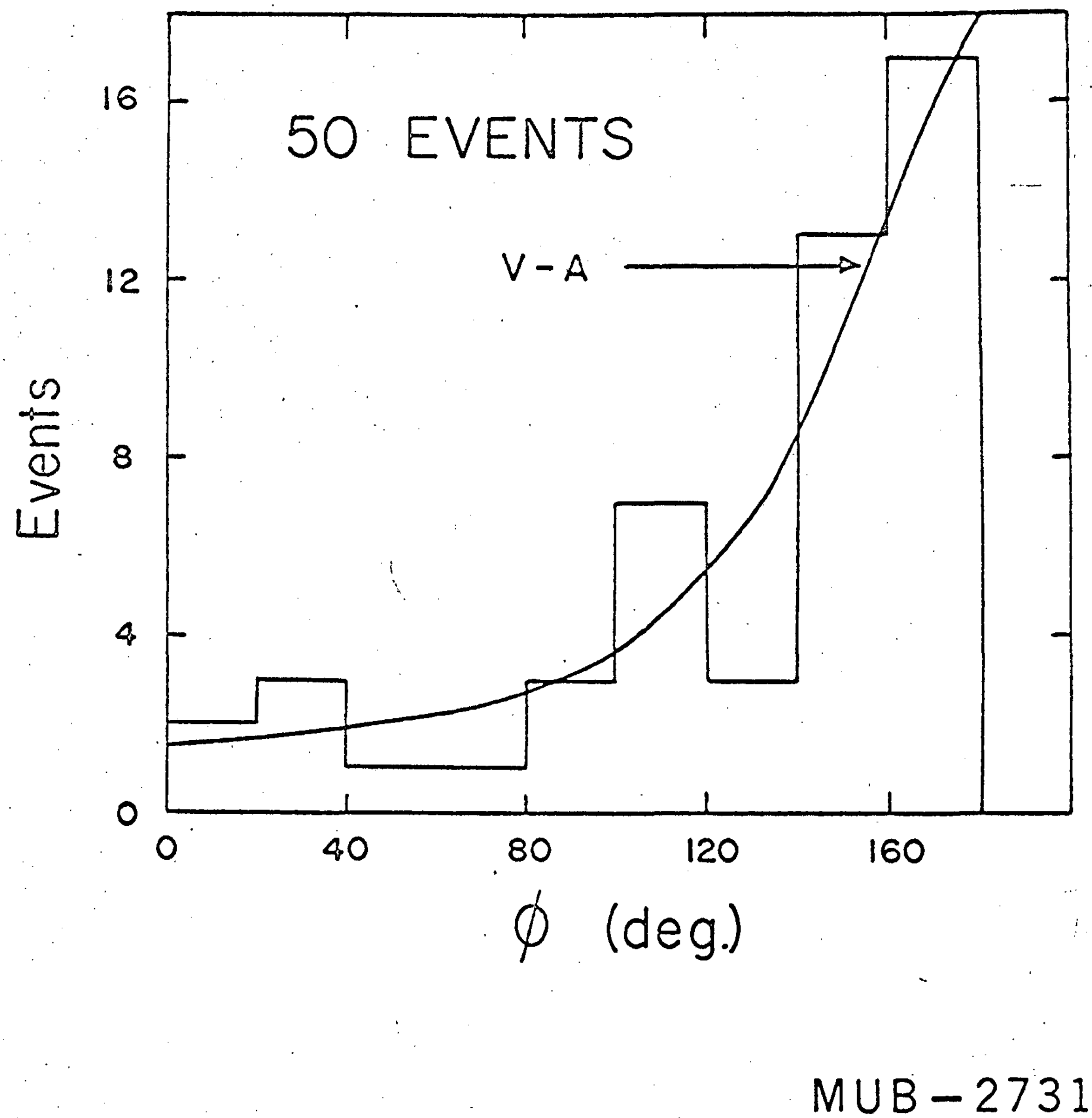

Fig. 16 Distribution of Φ (angle between proton and electron in Λ transverse plane) for 50 R_{max} Λ_β decays. V-A curve has experimental effects folded in.

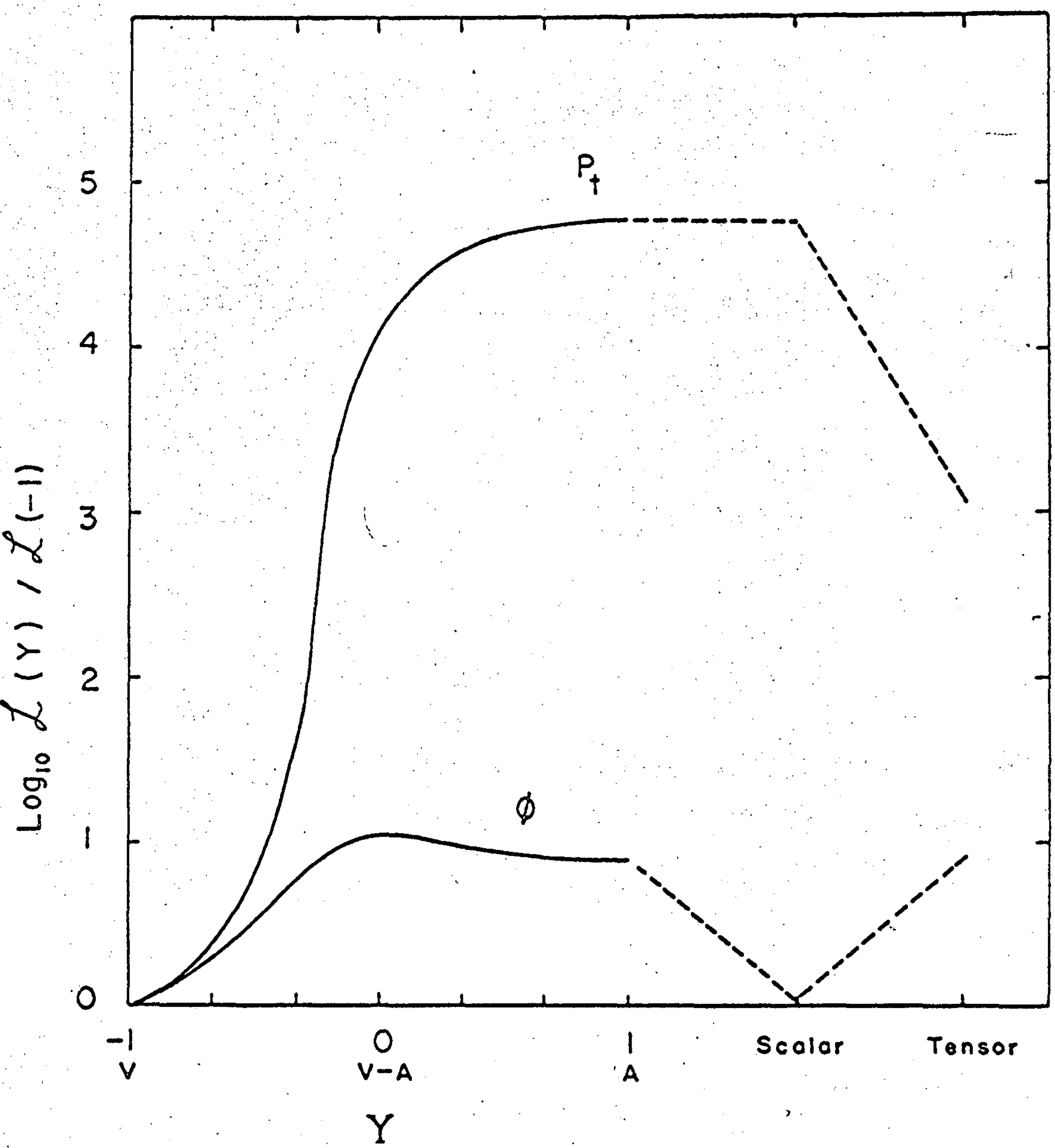

MUB-2748

Fig. 17 Likelihood curves for P_t and Φ data.
$Y = (|C_A| - |C_V|) / (|C_A| + |C_V|)$

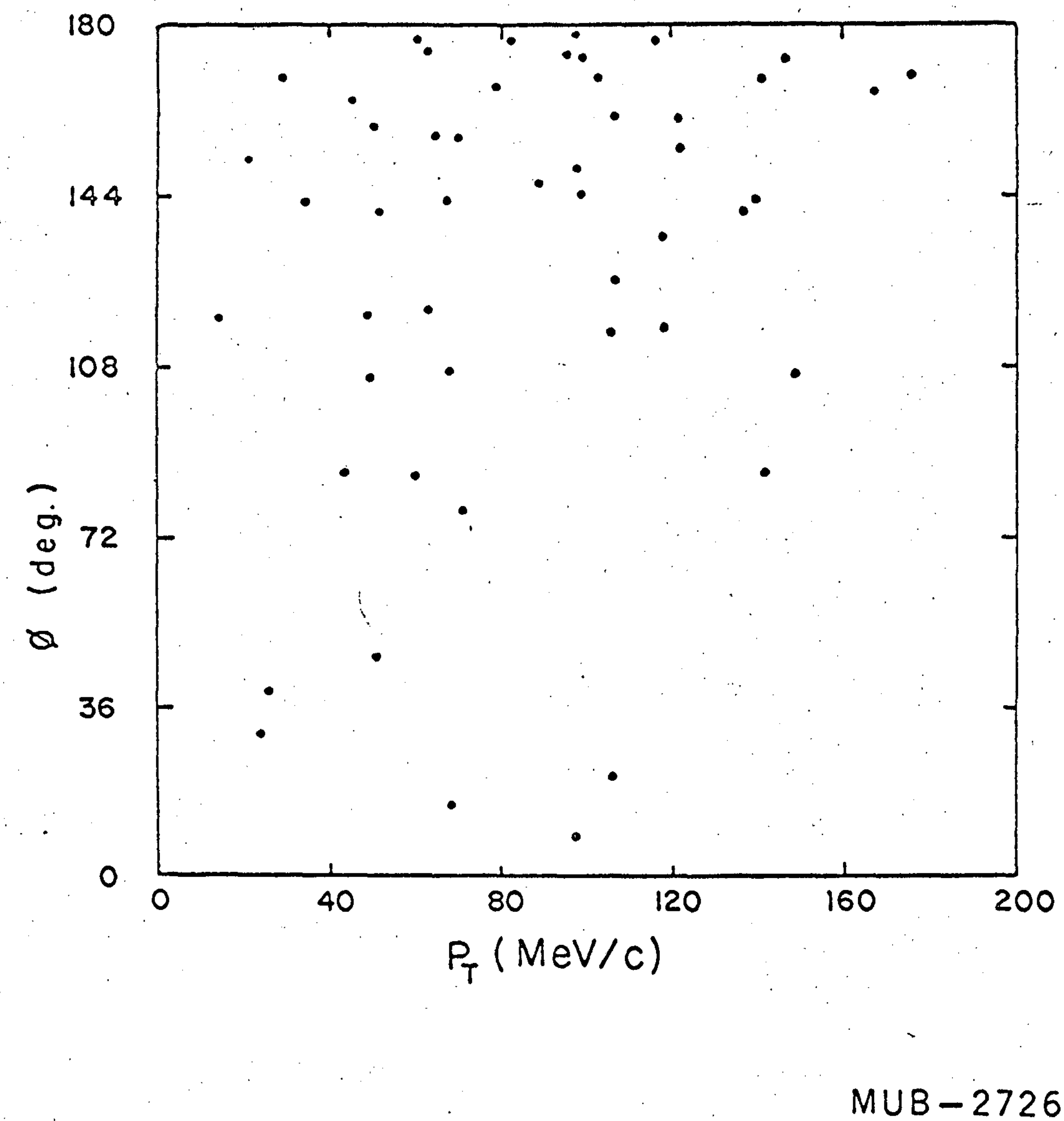

Fig. 18 Scatter diagram of Φ vs. P_t for 50 R_{max} Λ_β decays.

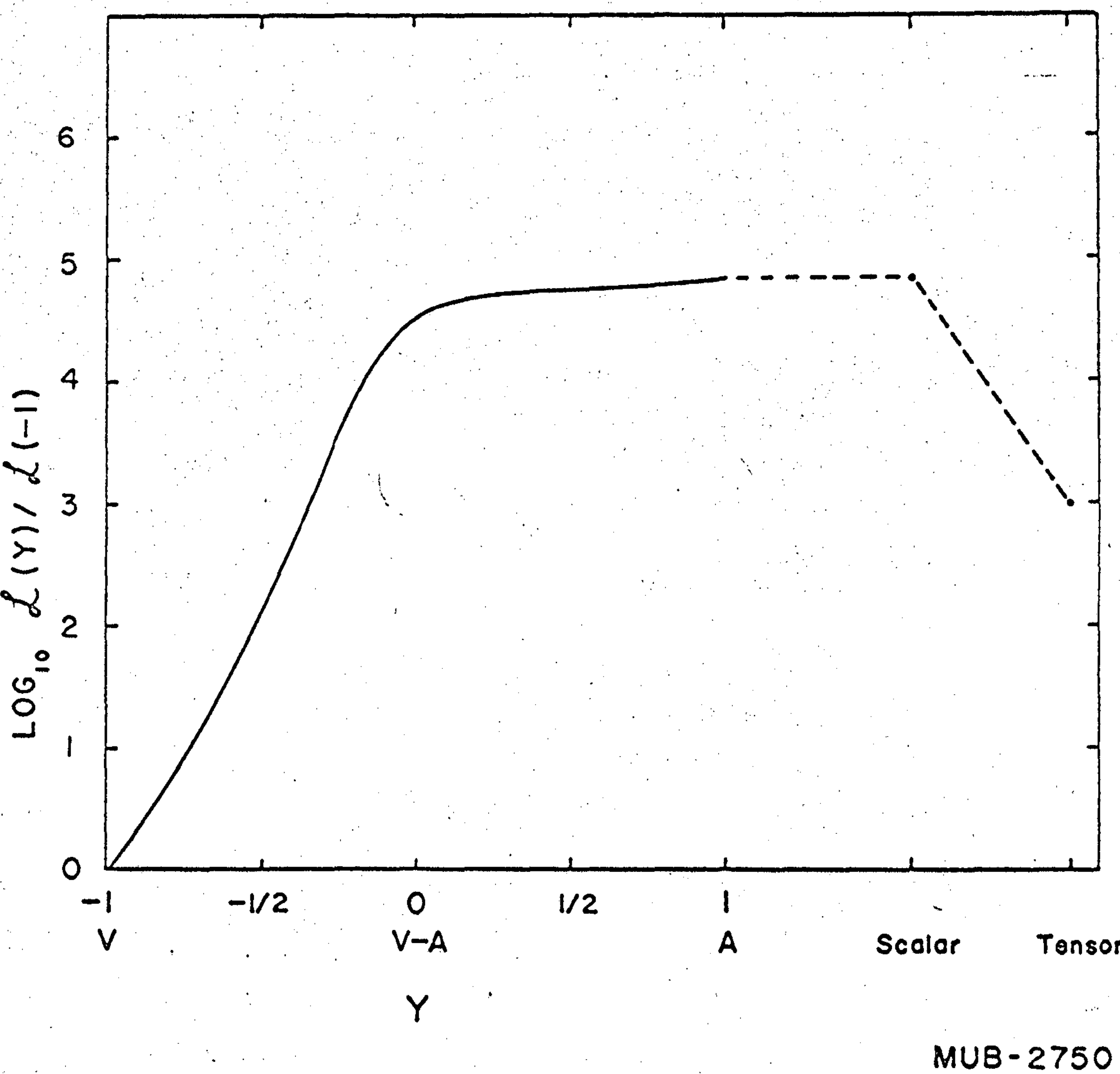

Fig. 19 Likelihood curve from combined P_t and Φ data.
$Y = (|C_A| - |C_V|) / (|C_A| + |C_V|)$

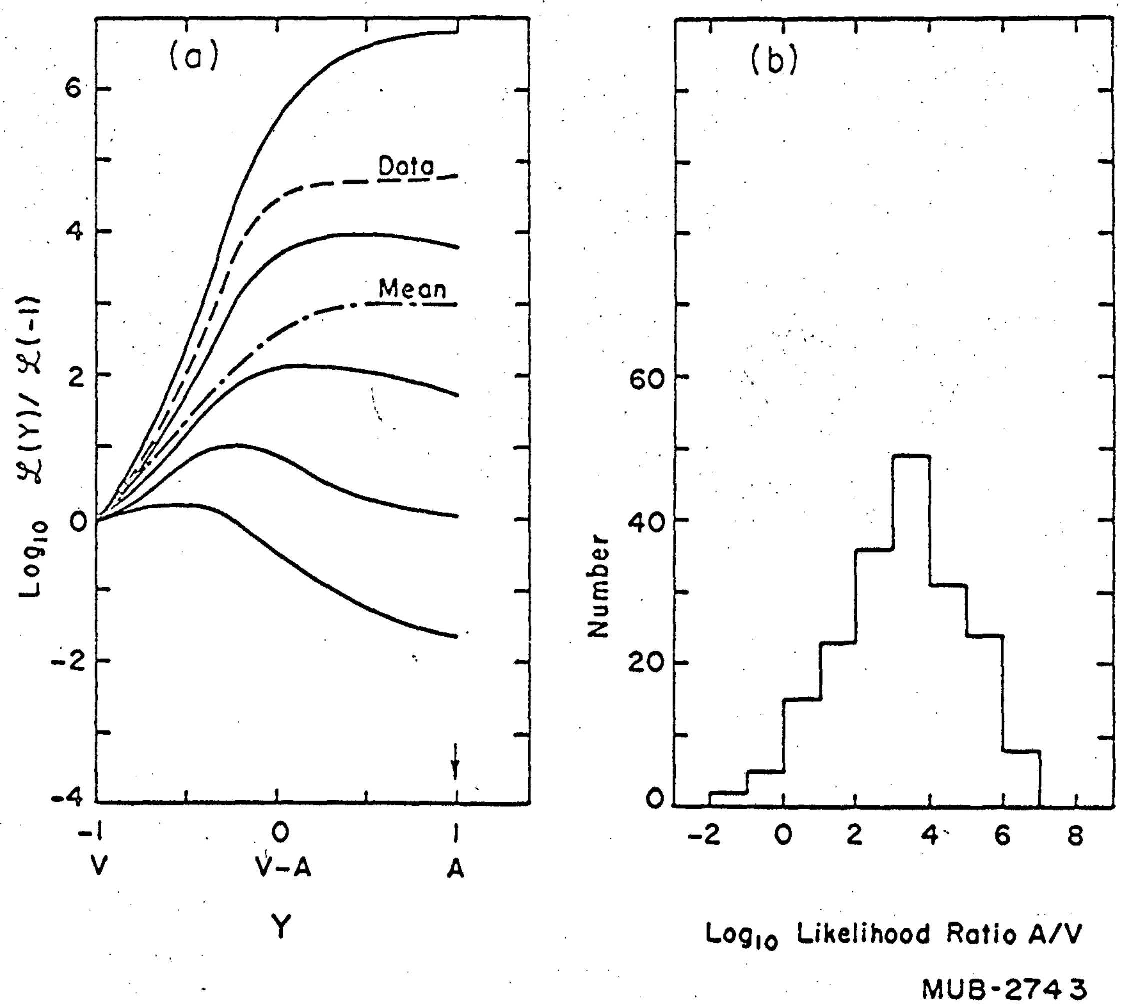

Fig. 20 (a) Likelihood curves from Monte Carlo experiments using a pure axial vector matrix element; experimental data shown for comparison.
(b) Distribution of $\log_{10}$ likelihood ratio A/V from all 200 Monte Carlo experiments.

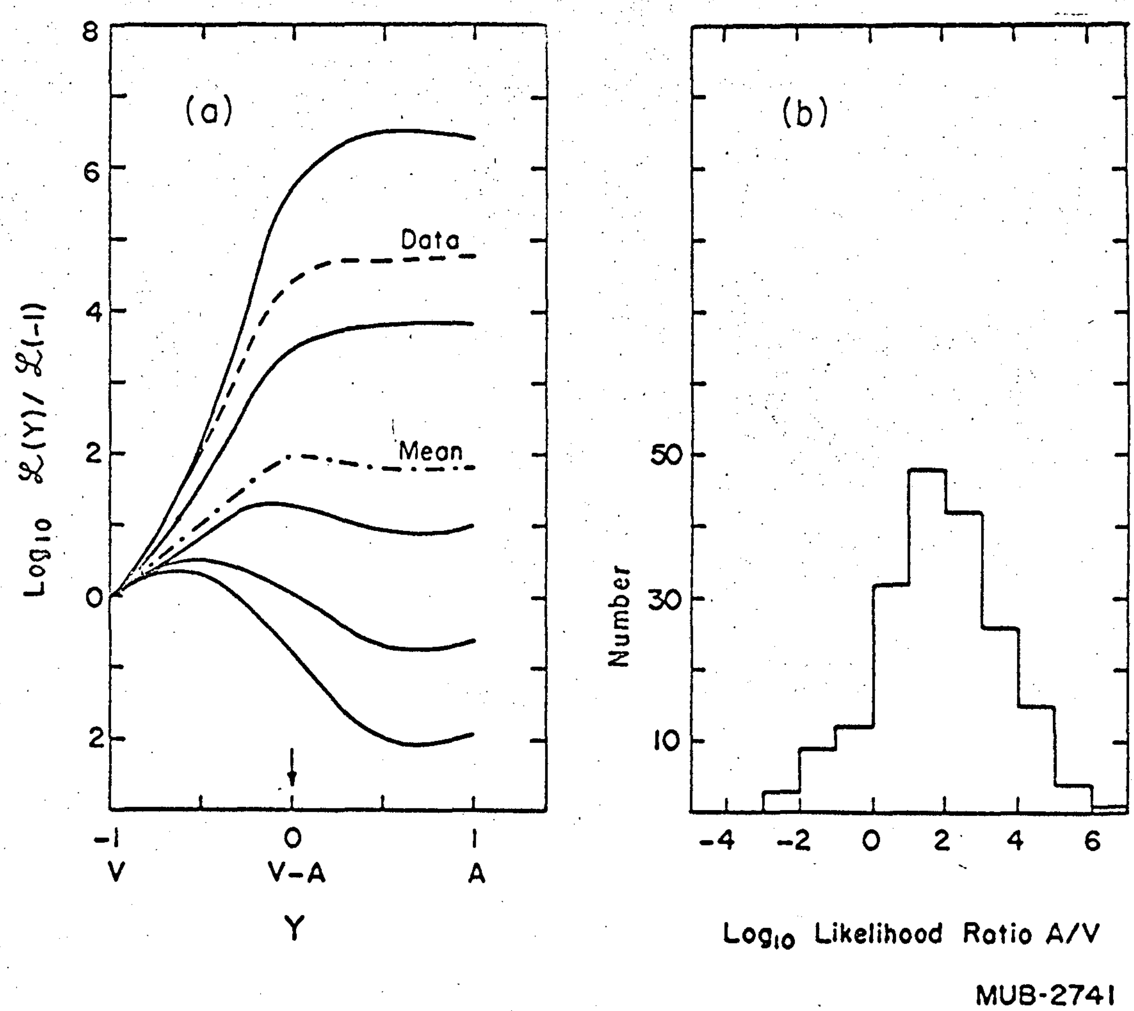

Fig. 21 (a) Likelihood curves from Monte Carlo experiments using a V-A matrix element; experimental data shown for comparison. (b) Distribution of $\log_{10}$ likelihood ratio A/V from all 200 Monte Carlo experiments.

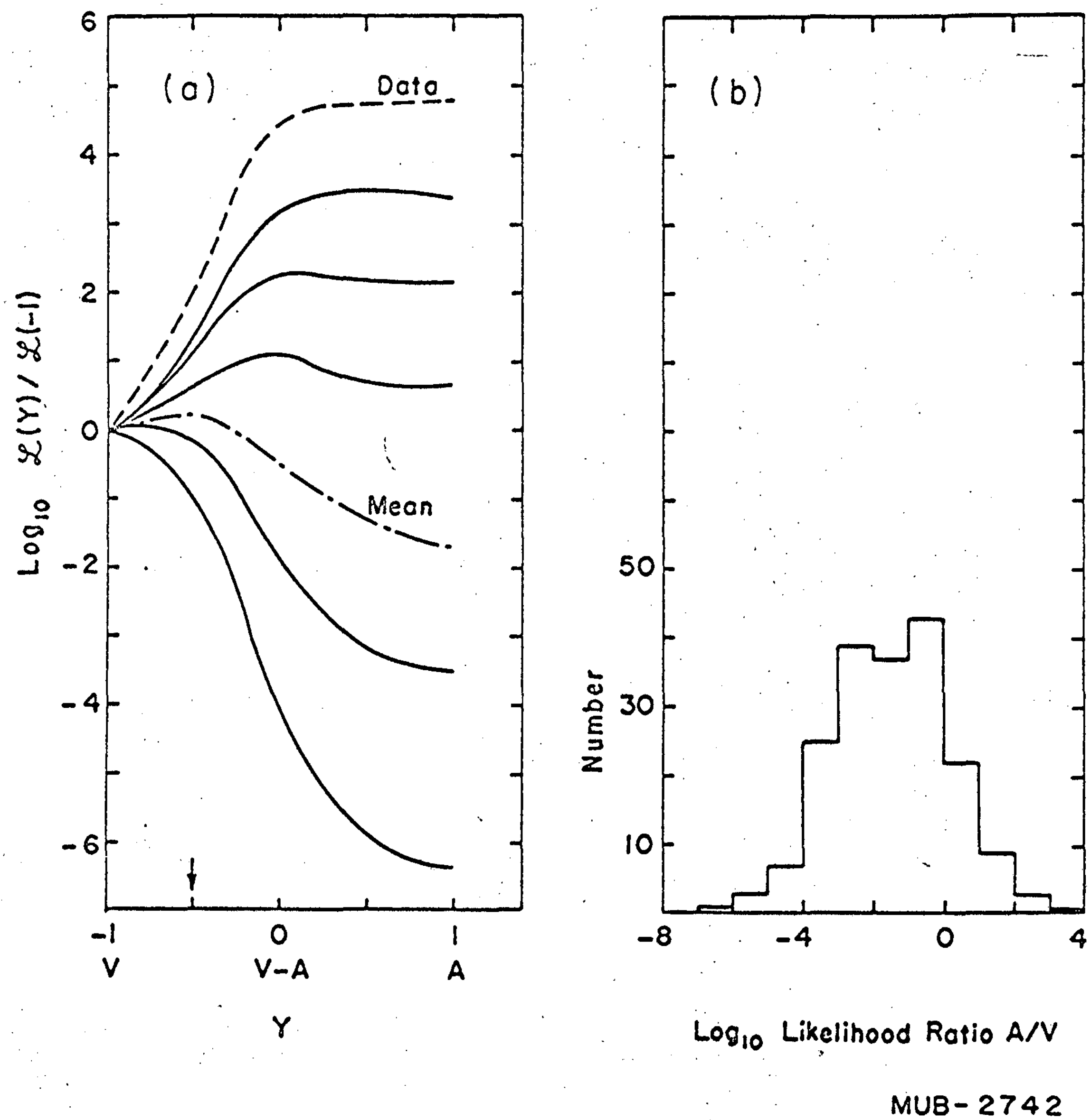

Fig. 22 (a) Likelihood curves from Monte Carlo experiments using a V-.33A matrix element; experimental data shown for comparison. (b) Distribution of $\log_{10}$ likelihood ratio A/V from all 200 Monte Carlo experiments.

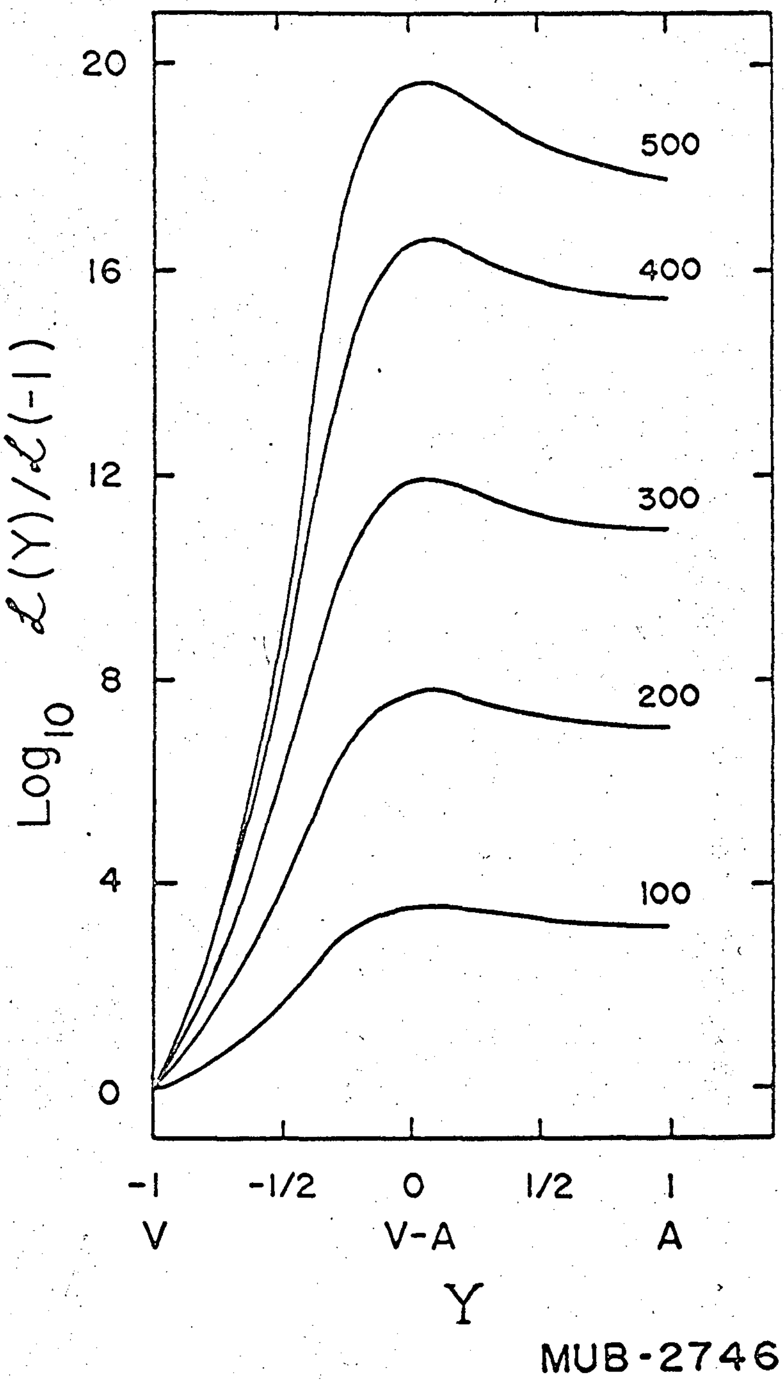

Fig. 23 Expected likelihood curves from experiments involving 100, 200, 300, 400, and 500 Λ_β decays using P_t and Φ only.

[illegible] [illegible]